

ESI for

Bis-triazolium containing macrocycles, pseudorotaxanes and interlocked structures for anion recognition

*Nicholas G. White, Henry G. Lovett & Paul D. Beer**

Contents	1
Details of instrumentation	2
NMR Spectra of new compounds	3
Synthesis and characterisation of additional compounds	22
ROESY NMR Spectra of 8·Cl⁻·10, 5·SO₄²⁻·8 and 22·(PF₆)₂	32
Titration protocols and additional binding isotherms	34
Comments on X-ray crystallography	37
References	38

Details of instrumentation

Routine NMR spectra were recorded on a Varian Mercury 300 spectrometer with ^1H NMR operating at 300 MHz, ^{13}C at 75.5 MHz, ^{19}F at 283 MHz, and ^{31}P at 122 MHz. Some compounds were too poorly-soluble, or not enough compound was synthesized to allow ^{13}C NMR spectra to be recorded on the 300 MHz spectrometer. In these cases, the spectra were collected on a Bruker AVII 500 spectrometer with a 5 mm $^{13}\text{C}(^1\text{H})$ dual cryoprobe with ^{13}C operating at 126 MHz and ^1H operating at 500 MHz.

High resolution ESI mass spectra were recorded on a Bruker μTOF spectrometer. High resolution EI mass spectra were recorded on a Waters GCT Classic spectrometer. Low resolution ESI mass spectra were recorded on a Waters LCT premier spectrometer.

NMR Spectra of new compounds

NMR Spectra of polyether bis-azide **1**

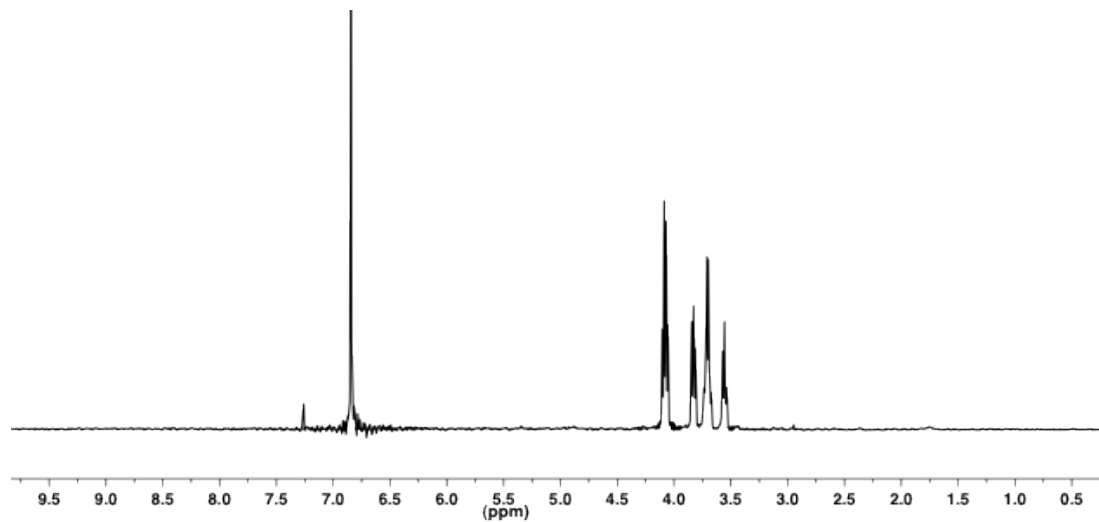


Figure S1. ^1H NMR spectrum of **1** (CDCl_3 , 293 K, 300 MHz).

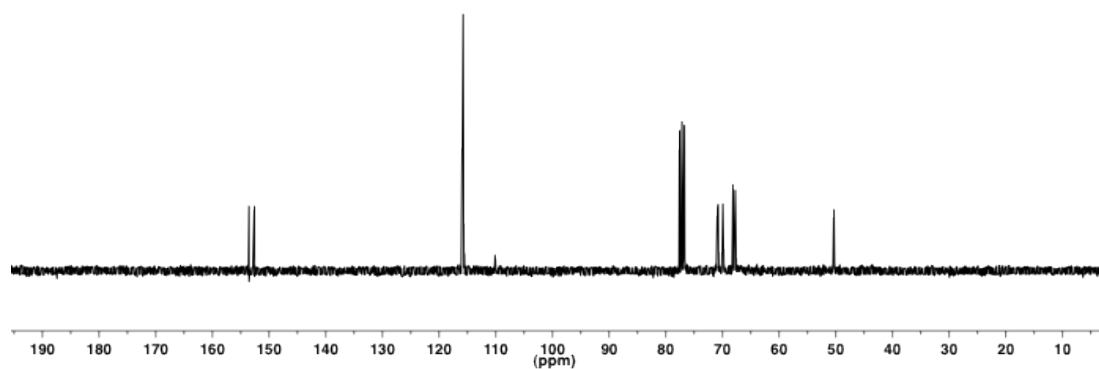


Figure S2. ^{13}C NMR spectrum of **1** (CDCl_3 , 293 K, 76 MHz).

NMR Spectra of phenyl bis-triazole macrocycle **3**

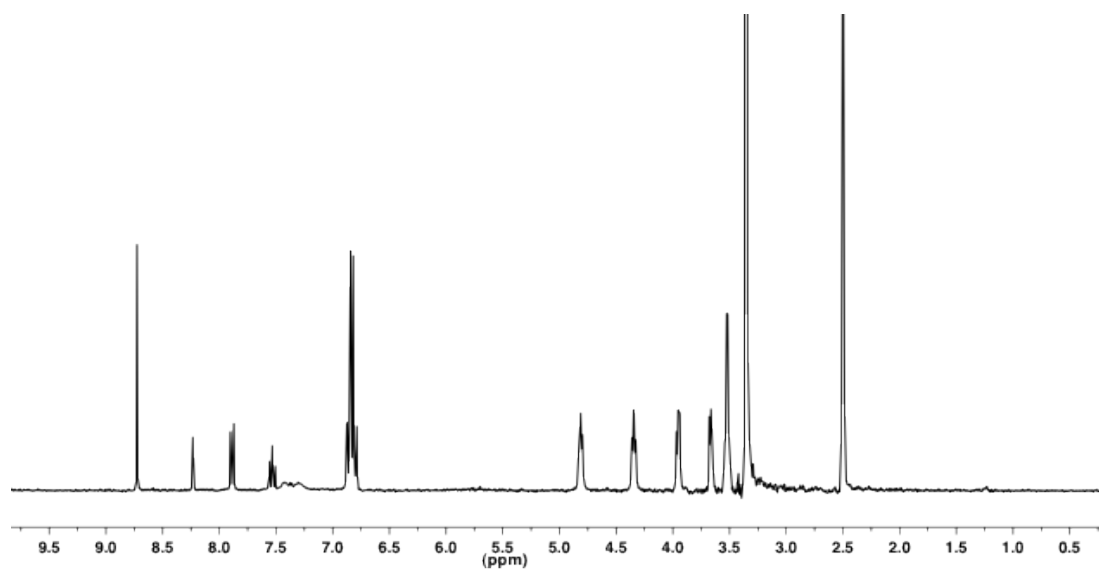


Figure S3. ¹H NMR spectrum of **3** (d₆-acetone, 293 K, 500 MHz).

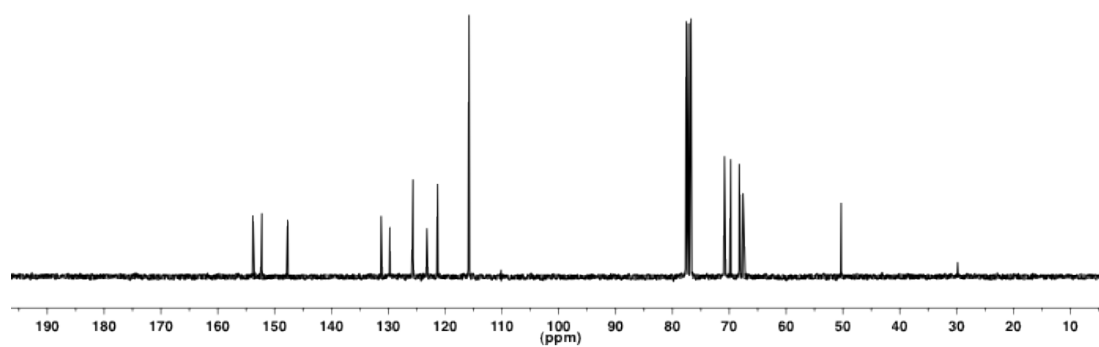


Figure S4. ¹³C NMR spectrum of **3** (CDCl₃, 293 K, 76 MHz).

NMR Spectra of propyl bis-triazole macrocycle **4**

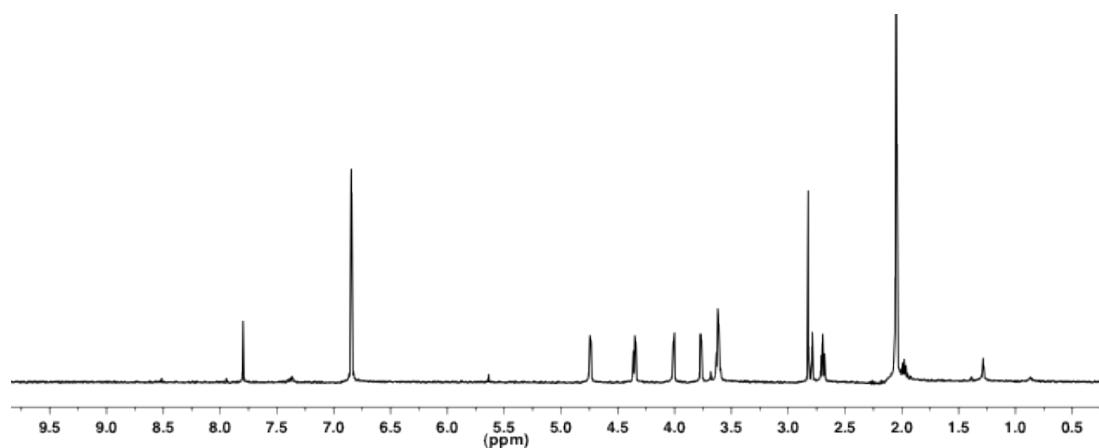


Figure S5. ^1H NMR spectrum of **4** (d_6 -acetone, 293 K, 500 MHz).

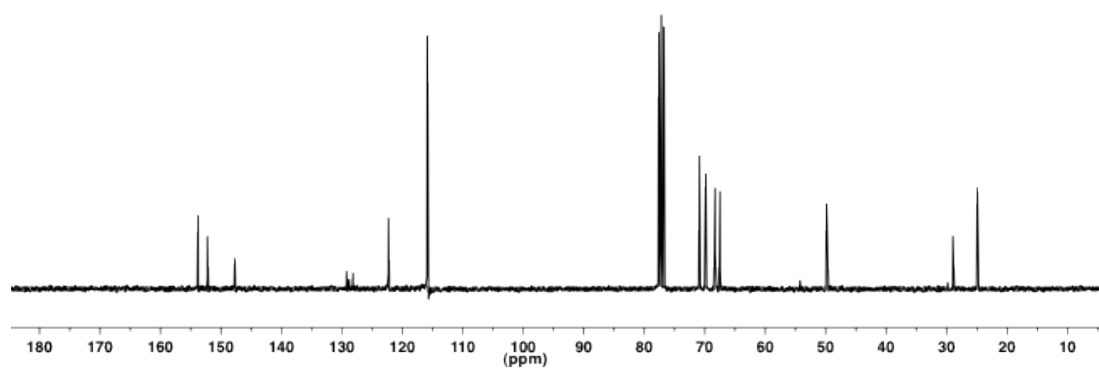


Figure S6. ^{13}C NMR spectrum of **4** (CDCl_3 , 293 K, 76 MHz).

NMR Spectra of bis-triazolium macrocycle $5 \cdot (\text{BF}_4)_2$

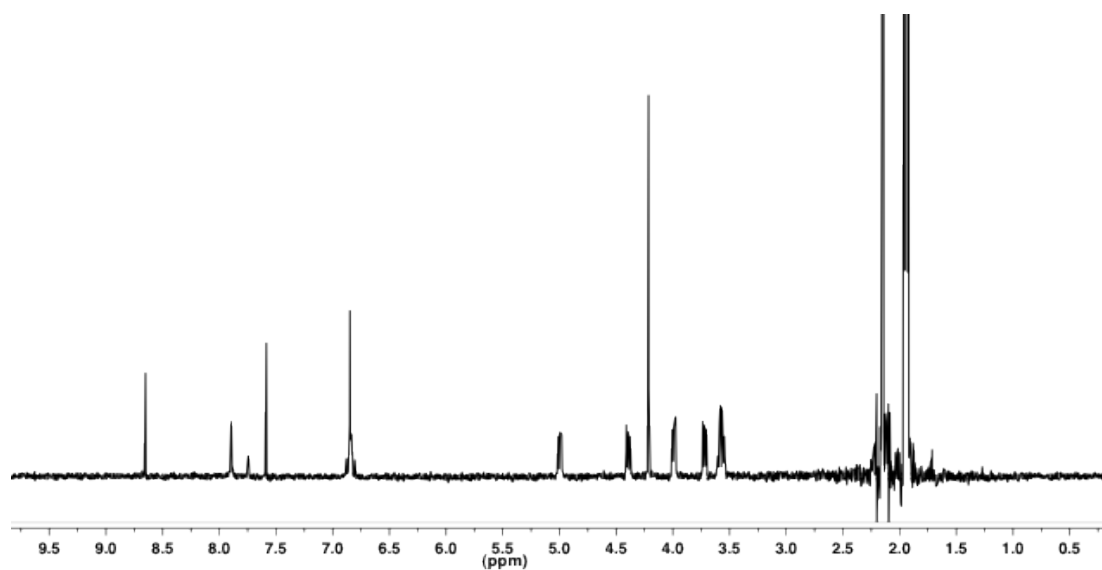


Figure S7. ^1H NMR spectrum of $5 \cdot (\text{BF}_4)_2$ (CD_3CN , 293 K, 300 MHz).

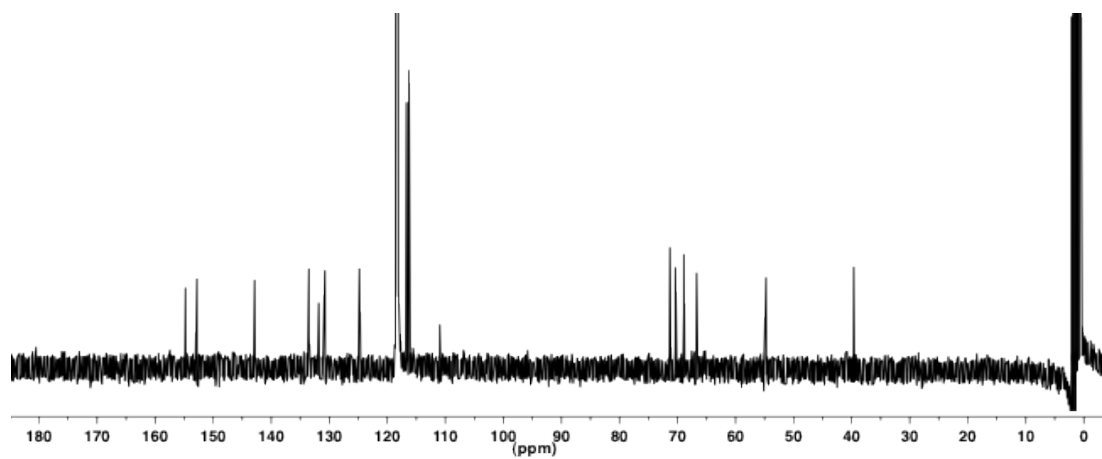


Figure S8. ^{13}C NMR spectrum of $5 \cdot (\text{BF}_4)_2$ (CD_3CN , 293 K, 76 MHz).

NMR Spectra of phenyl bis-triazole thread **6**

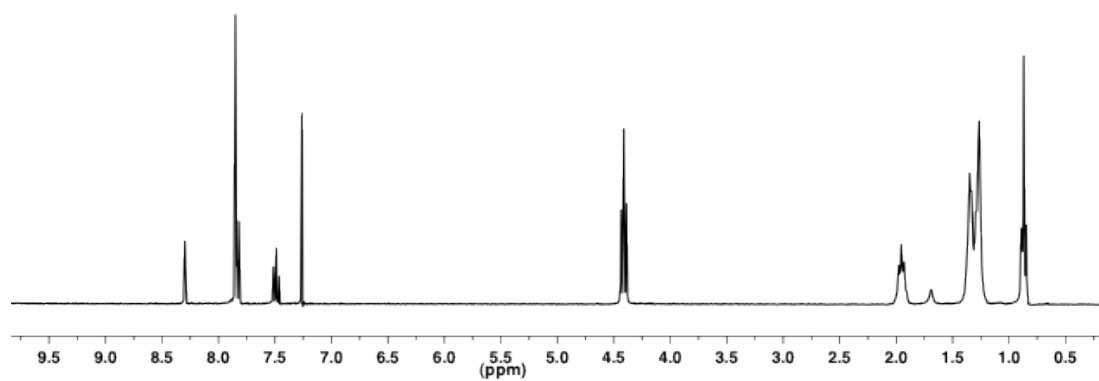


Figure S9. ¹H NMR spectrum of **6** (CDCl₃, 293 K, 300 MHz).

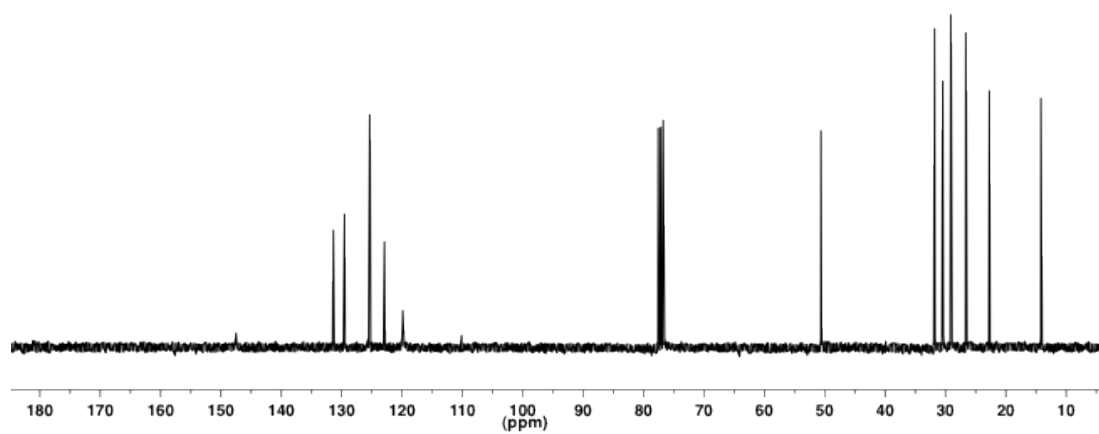


Figure S10. ¹³C NMR spectrum of **6** (CDCl₃, 293 K, 76 MHz).

NMR Spectra of propyl bis-triazole thread 7

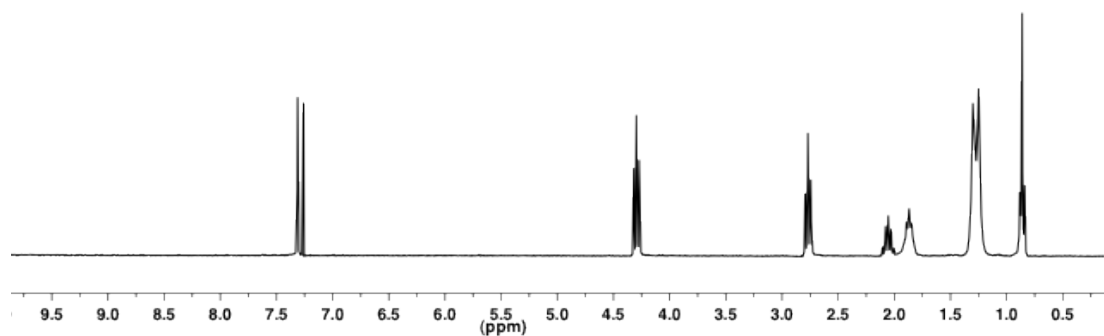


Figure S11. ^1H NMR spectrum of **7** (CDCl_3 , 293 K, 300 MHz).

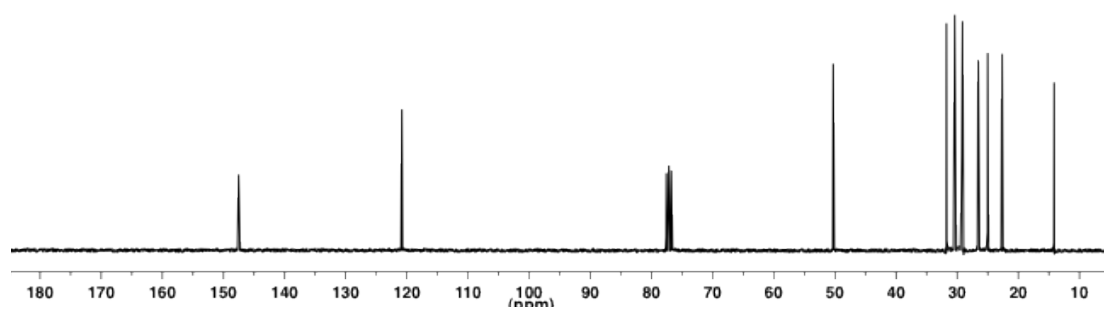


Figure S12. ^{13}C NMR spectrum of **7** (CDCl_3 , 293 K, 76 MHz).

NMR Spectra of phenyl bis-triazolium thread $8 \cdot (\text{BF}_4)_2$

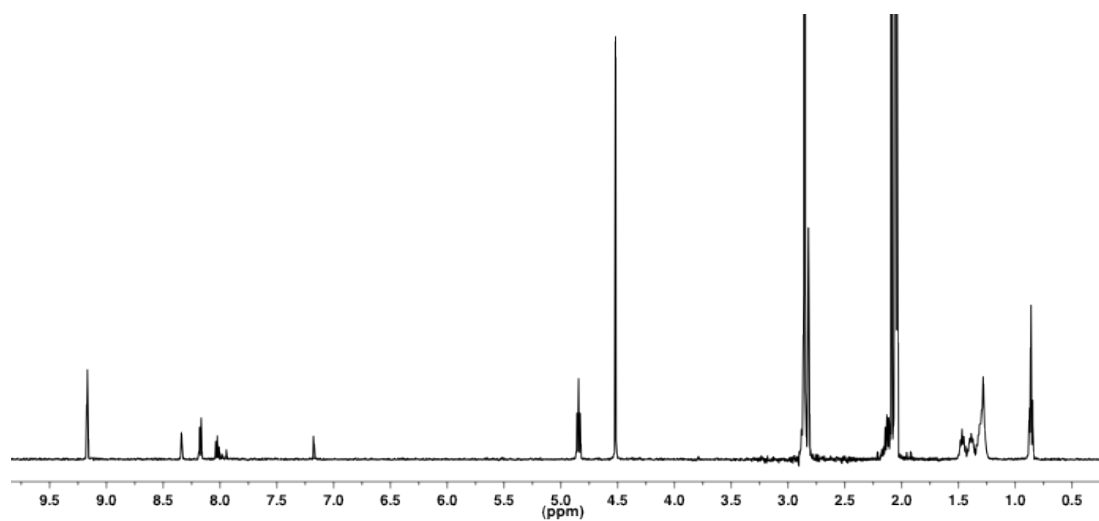


Figure S13. ^1H NMR spectrum of $8 \cdot (\text{BF}_4)_2$ (d_6 -acetone, 293 K, 500 MHz).

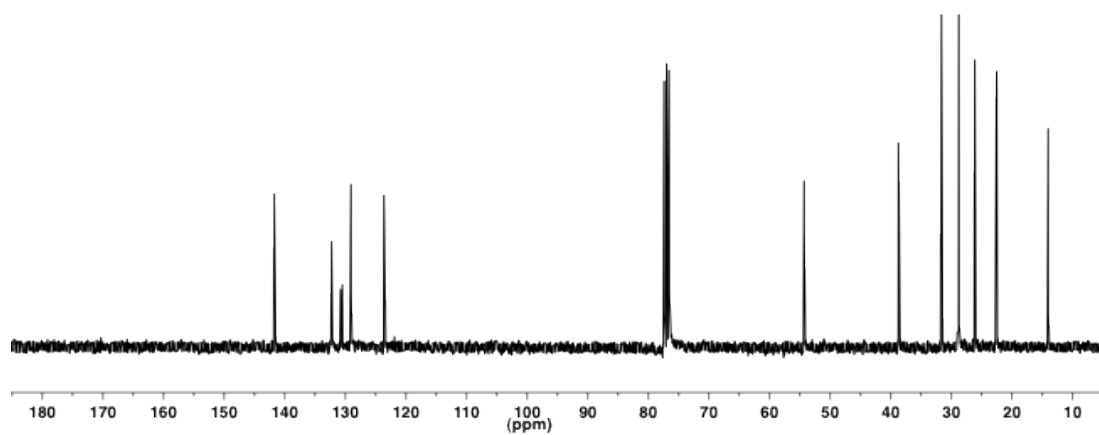


Figure S14. ^{13}C NMR spectrum of $8 \cdot (\text{BF}_4)_2$ (CDCl_3 , 293 K, 76 MHz).

NMR Spectra of propyl bis-triazolium thread $9 \cdot (\text{BF}_4)_2$

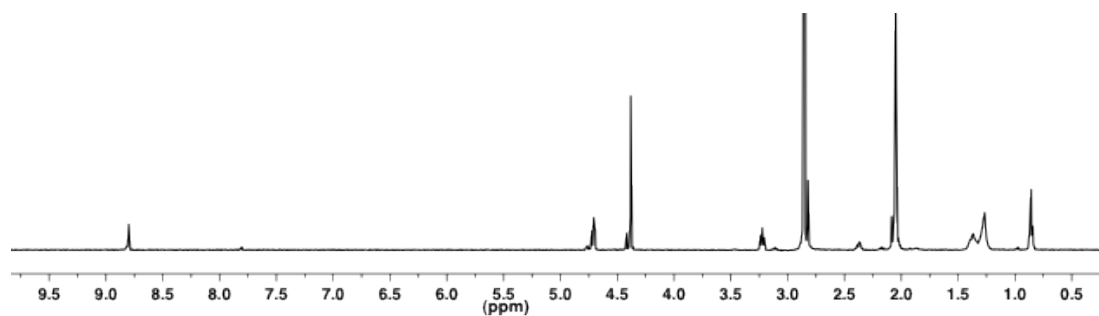


Figure S15. ^1H NMR spectrum of $9 \cdot (\text{BF}_4)_2$ (d_6 -acetone, 293 K, 500 MHz).

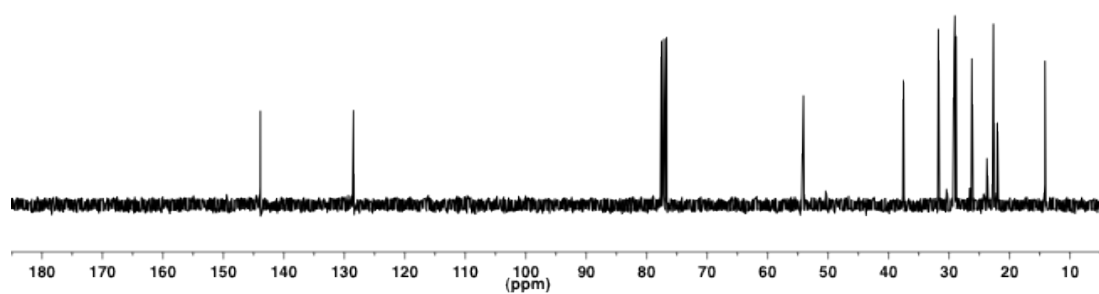


Figure S16. ^{13}C NMR spectrum of $9 \cdot (\text{BF}_4)_2$ (CDCl_3 , 293 K, 76 MHz).

NMR Spectra of phenyl bis-triazole axle **11**

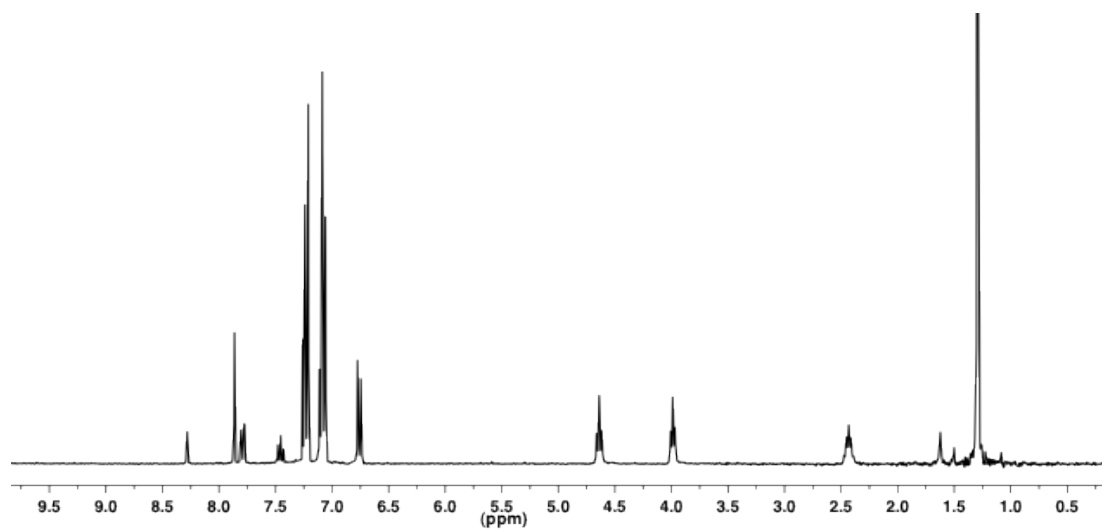


Figure S17. ^1H NMR spectrum of **11** (CDCl_3 , 293 K, 300 MHz).

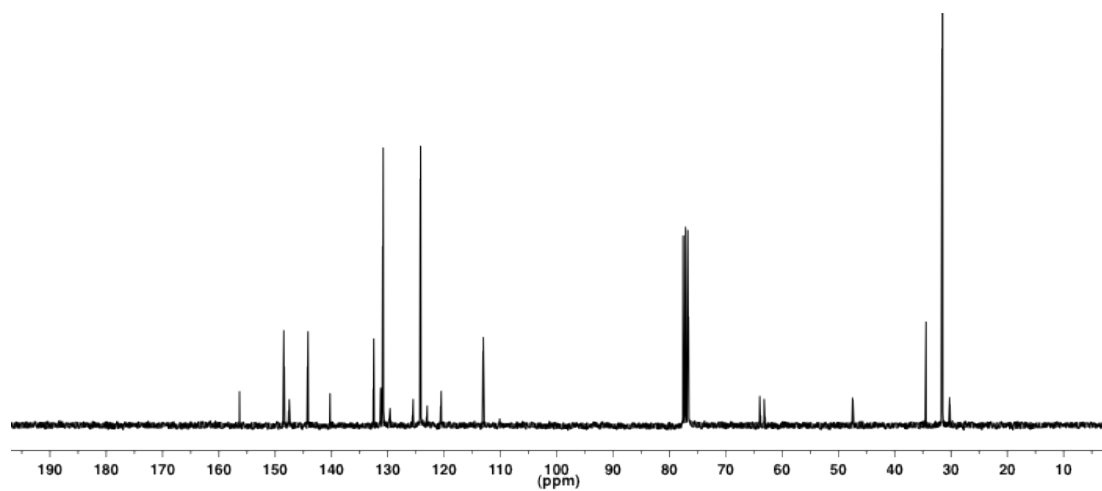


Figure S18. ^{13}C NMR spectrum of **11** (CDCl_3 , 293 K, 76 MHz).

NMR Spectra of propyl bis-triazole axle **12**

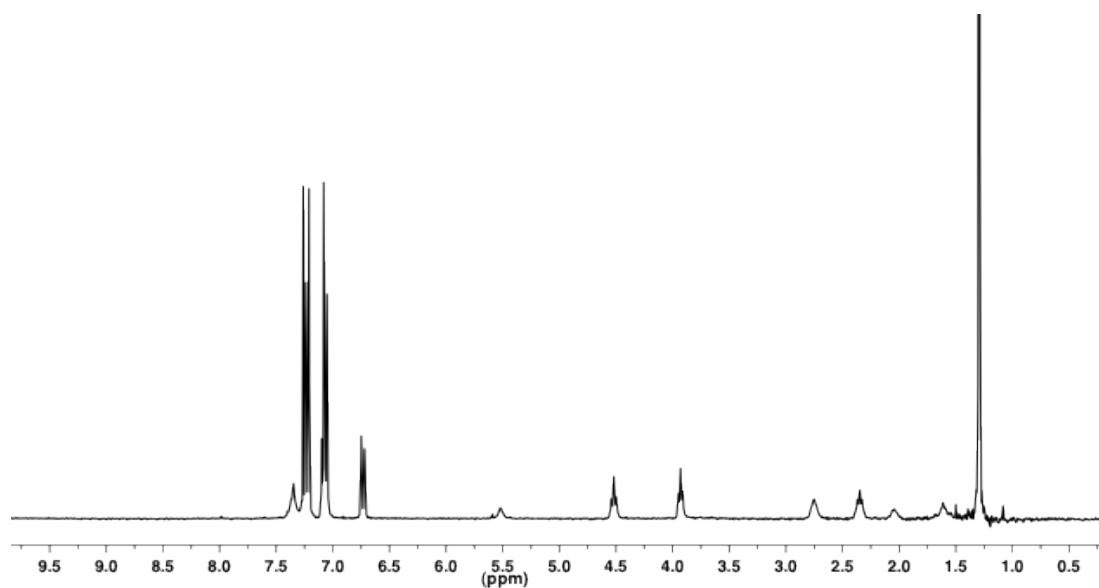


Figure S19. ¹H NMR spectrum of **12** (CDCl₃, 293 K, 300 MHz).

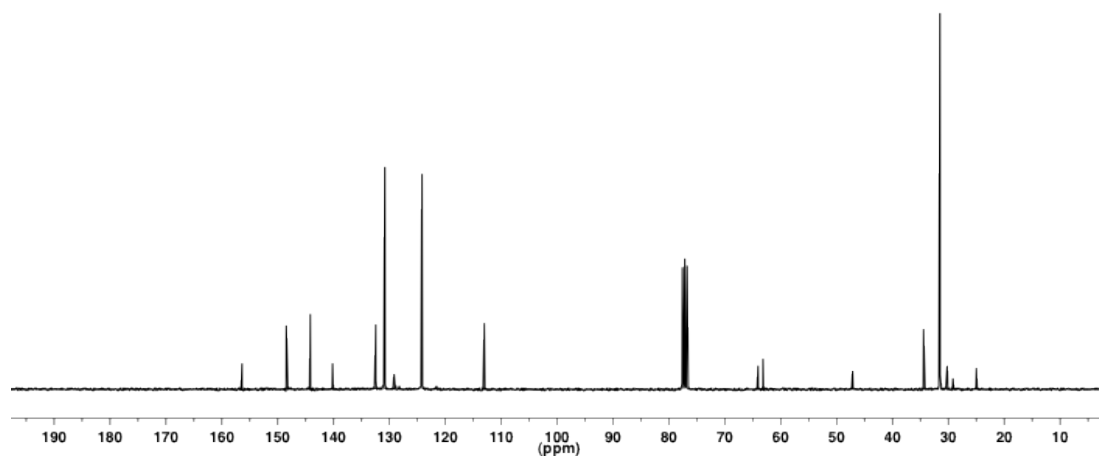


Figure S20. ¹³C NMR spectrum of **12** (CDCl₃, 293 K, 76 MHz).

NMR Spectra of phenyl bis-triazolium axle $14 \cdot (\text{BF}_4)_2$

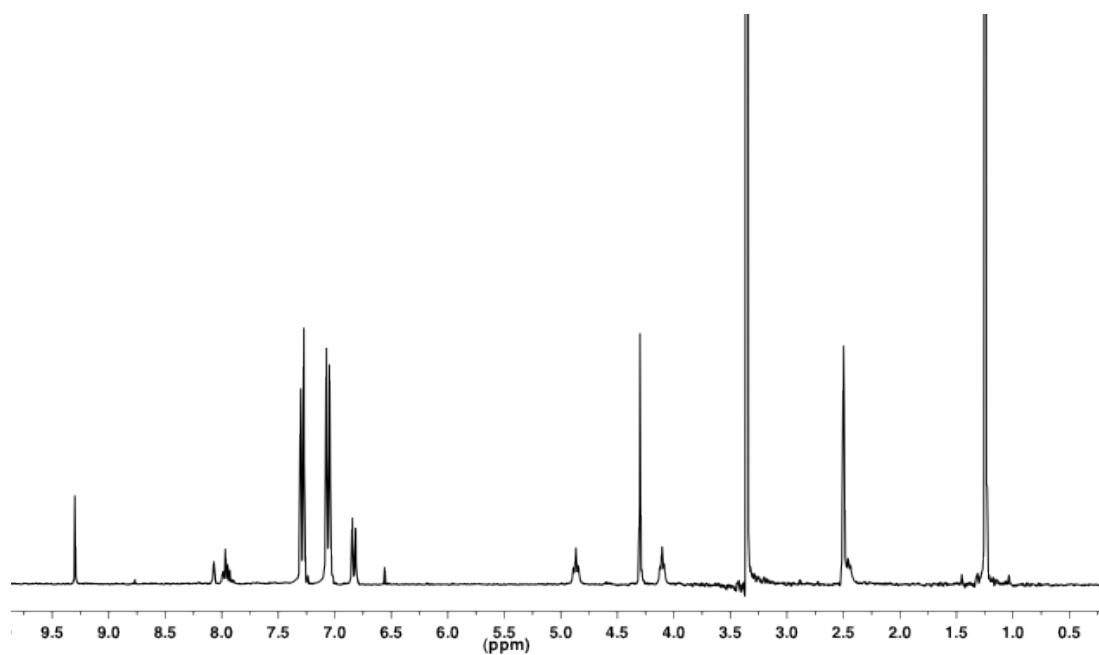


Figure S21. ^1H NMR spectrum of $14 \cdot (\text{BF}_4)_2$ (d_6 -DMSO, 293 K, 300 MHz).

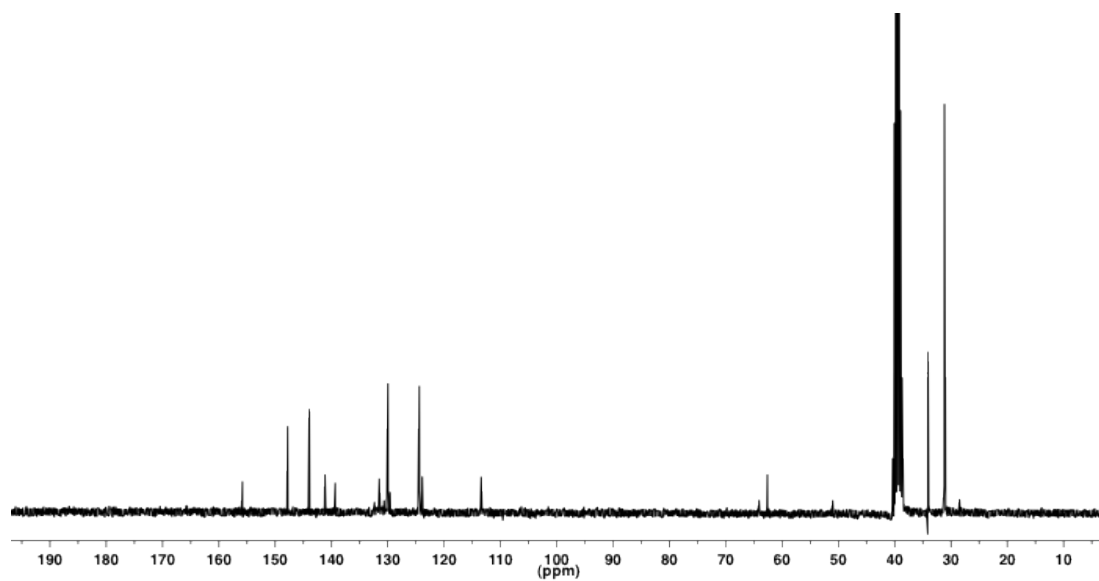


Figure S22. ^{13}C NMR spectrum of $14 \cdot (\text{BF}_4)_2$ (d_6 -DMSO, 293 K, 76 MHz).

NMR Spectra of propyl bis-triazolium axle $15 \cdot (\text{BF}_4)_2$

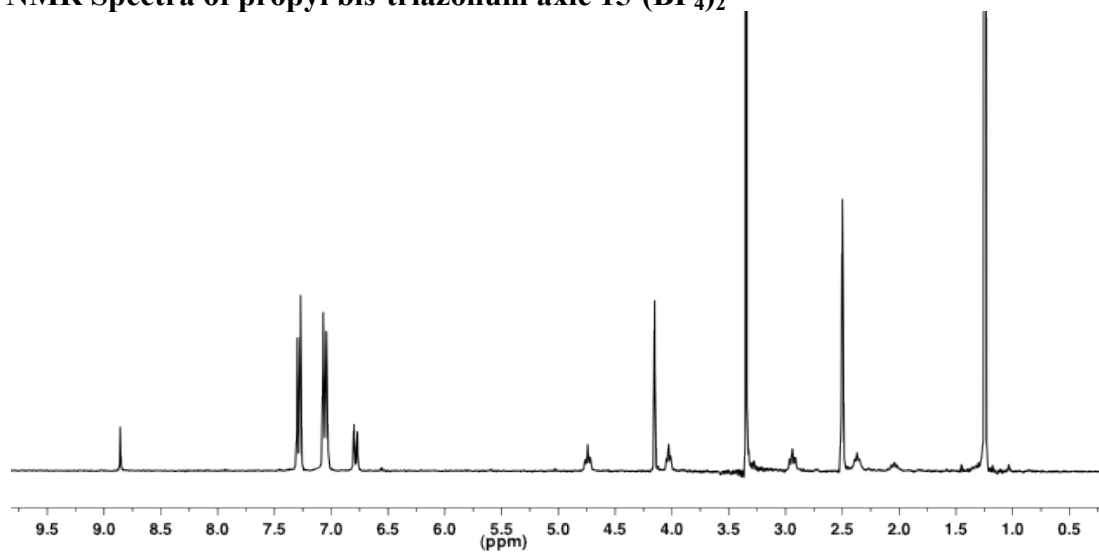


Figure S23. ^1H NMR spectrum of $15 \cdot (\text{BF}_4)_2$ (d_6 -DMSO, 293 K, 300 MHz).

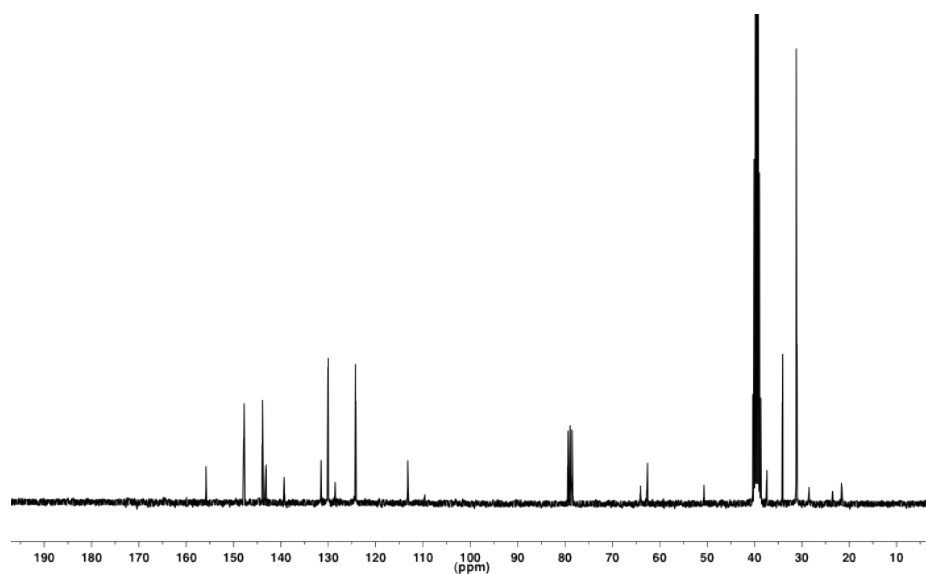


Figure S24. ^{13}C NMR spectrum of $15 \cdot (\text{BF}_4)_2$ (d_6 -DMSO, 293 K, 76 MHz).

NMR Spectra of bis(triazole xylyl azide) **19**

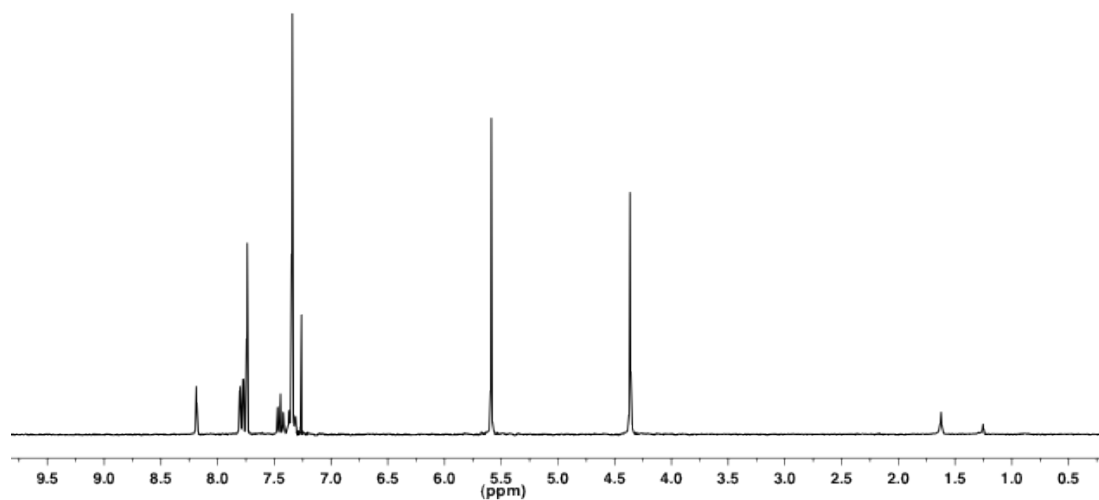


Figure S25. ¹H NMR spectrum of **19** (CDCl₃, 293 K, 300 MHz).

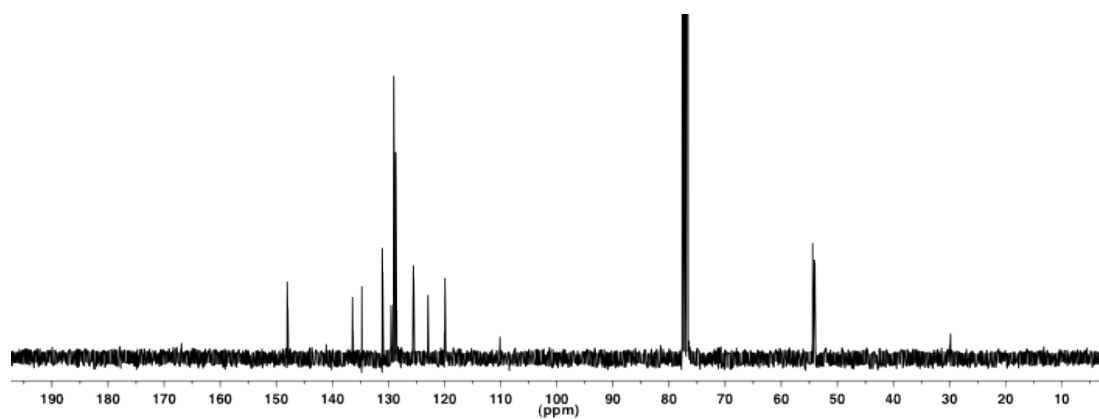


Figure S26. ¹³C NMR spectrum of **19** (CDCl₃, 293 K, 76 MHz).

NMR Spectra of bis(triazolium xylyl azide) $20 \cdot (\text{BF}_4)_2$

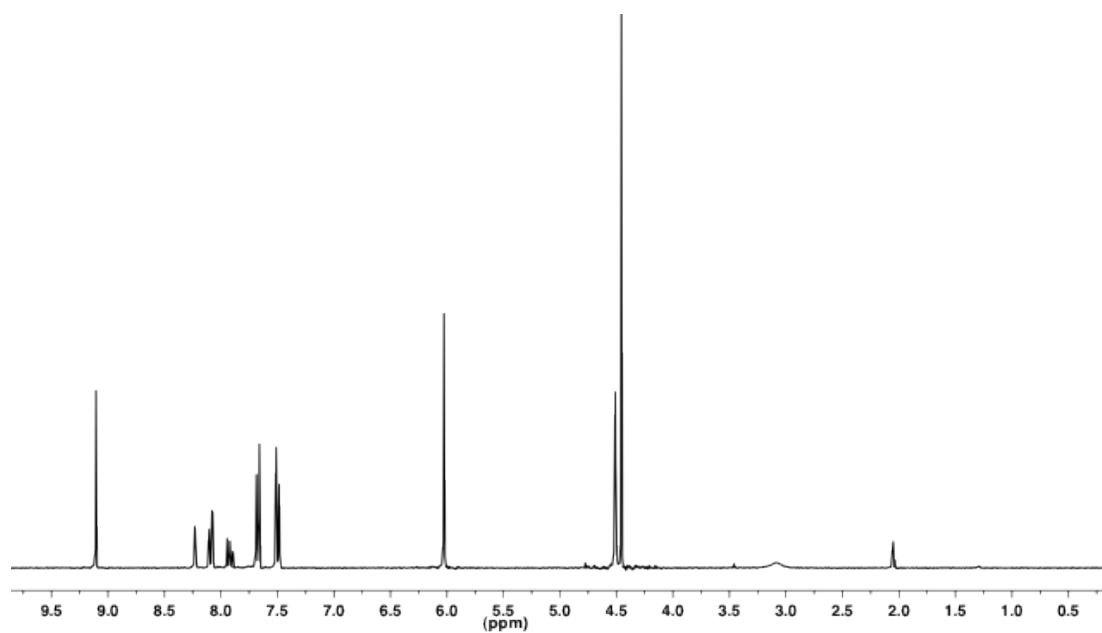


Figure S27. ^1H NMR spectrum of $20 \cdot (\text{BF}_4)_2$ (d_6 -acetone, 293 K, 300 MHz).

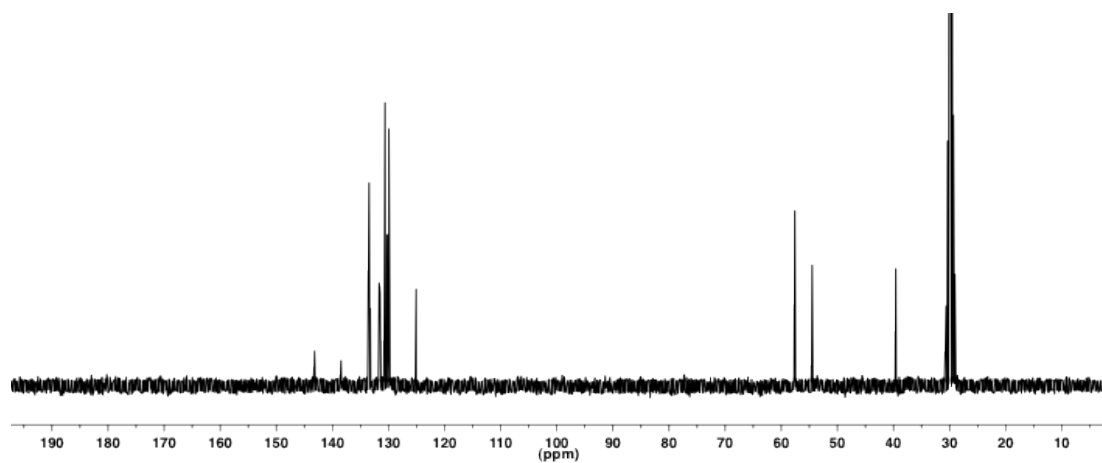


Figure S28. ^{13}C NMR spectrum of $20 \cdot (\text{BF}_4)_2$ (d_6 -acetone, 293 K, 76 MHz).

NMR Spectra of bis-triazolium rotaxane $22 \cdot (\text{PF}_6)_2$

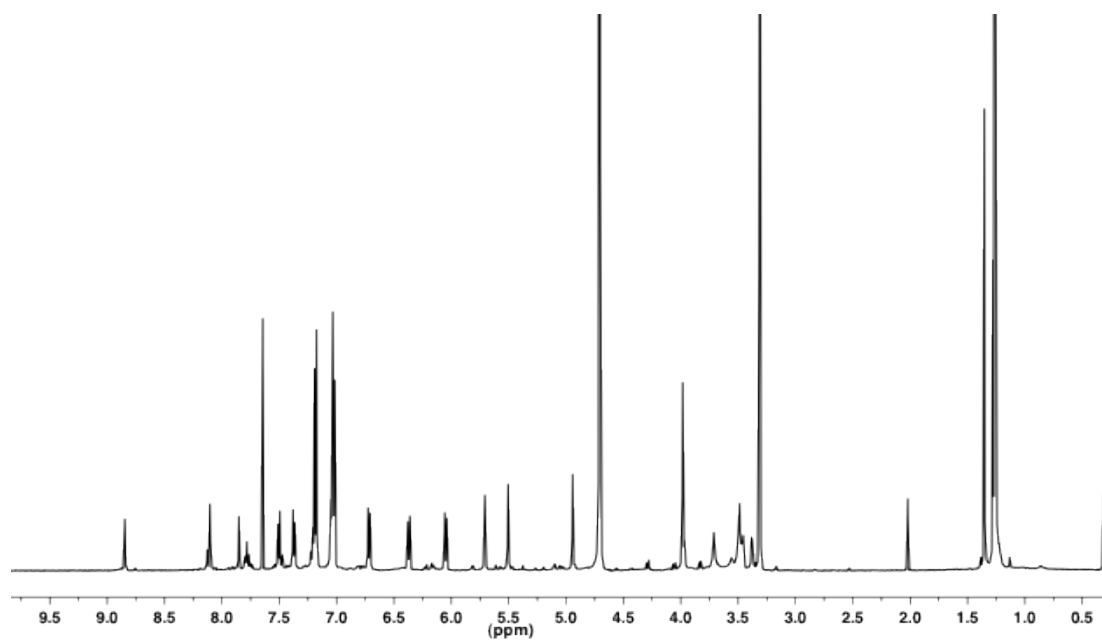


Figure S29. ^1H NMR spectrum of $22 \cdot (\text{PF}_6)_2$ (1:1 CDCl_3 : CD_3OD , 293 K, 500 MHz).

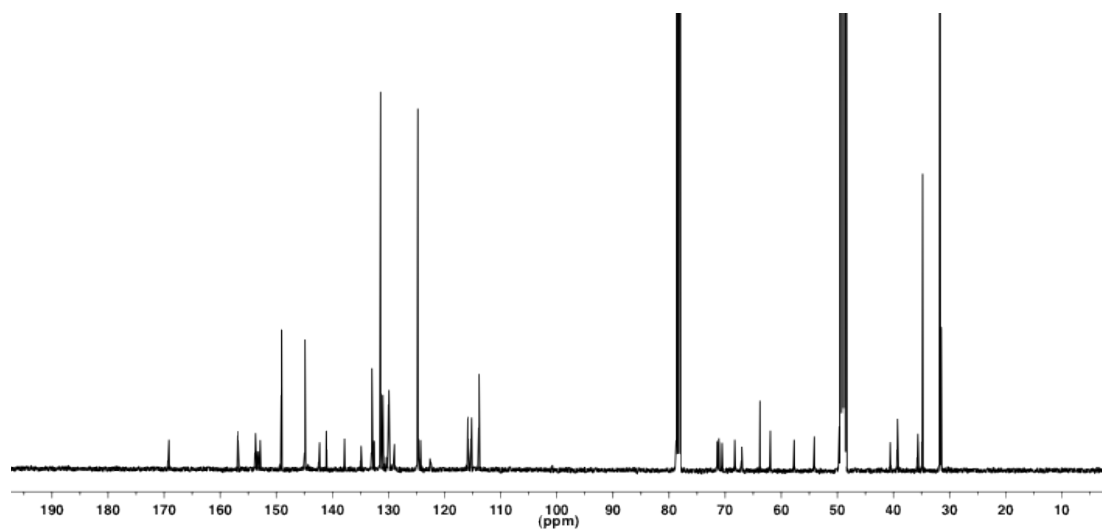


Figure S30. ^{13}C NMR spectrum of $22 \cdot (\text{PF}_6)_2$ (1:1 CDCl_3 : CD_3OD , 293 K, 126 MHz).

NMR Spectra of bis-triazole bis-azide **24**

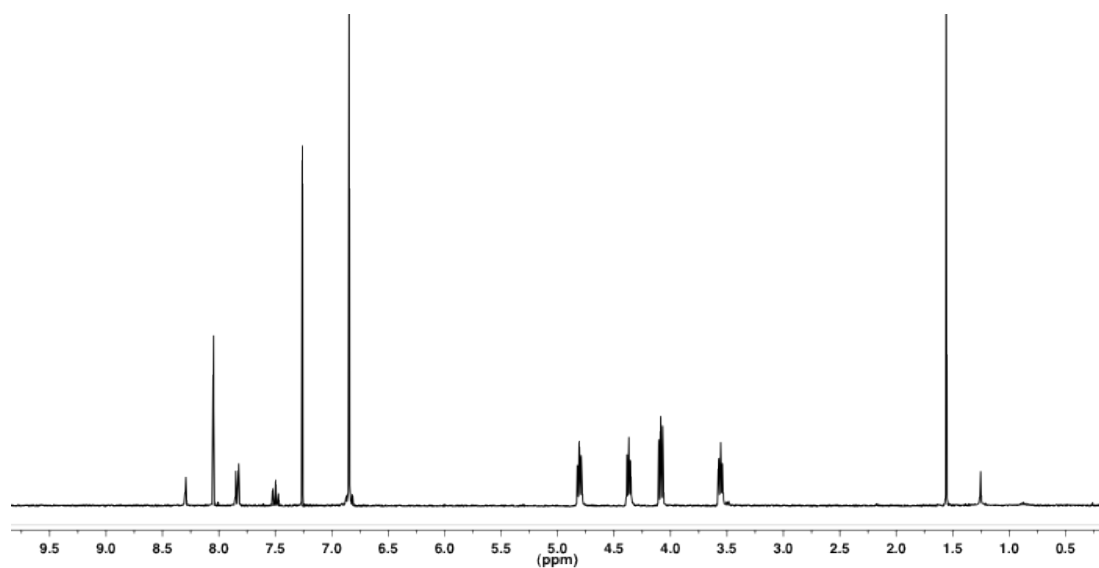


Figure S31. ^1H NMR spectrum of **24** (CDCl_3 , 293 K, 300 MHz).

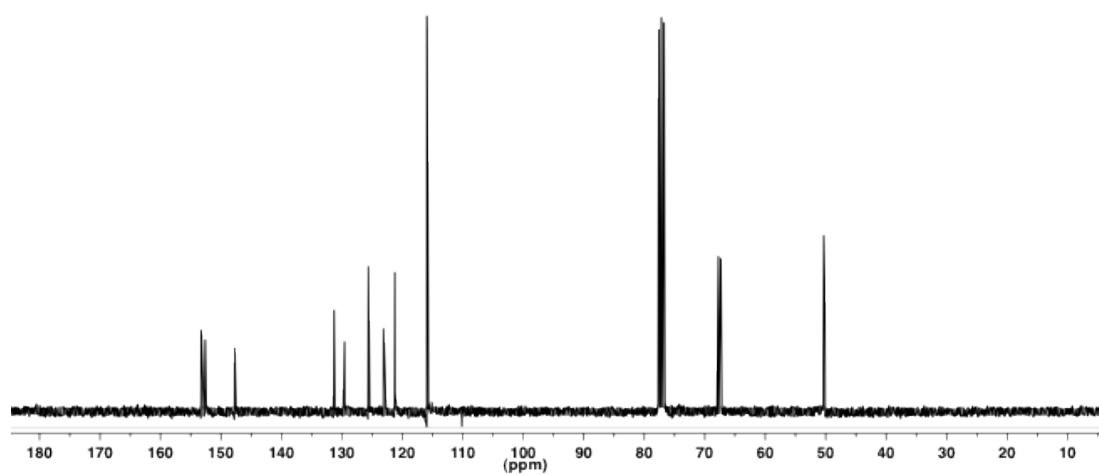


Figure S32. ^{13}C NMR spectrum of **24** (CDCl_3 , 293 K, 76 MHz).

NMR Spectra of bis-triazolium bis-azide $25 \cdot (\text{BF}_4)_2$

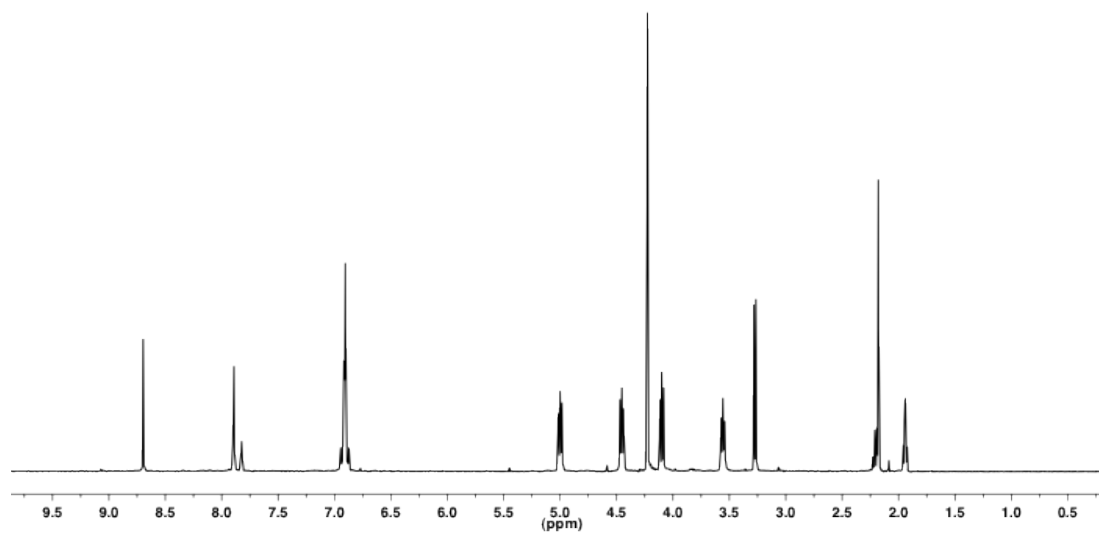


Figure S33. ^1H NMR spectrum of $25 \cdot (\text{BF}_4)_2$ (CD_3CN , 293 K, 300 MHz).

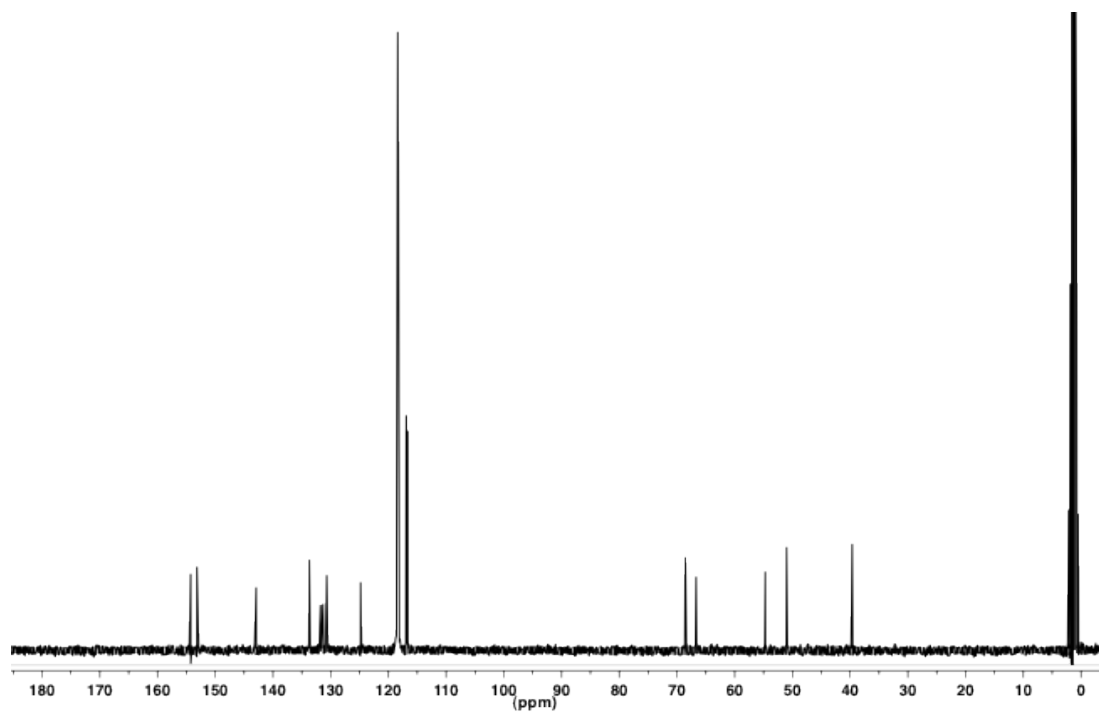


Figure S34. ^{13}C NMR spectrum of $25 \cdot (\text{BF}_4)_2$ (CD_3CN , 293 K, 76 MHz).

NMR Spectra of *hetero-catenane* **26**·(BPh₄)₄

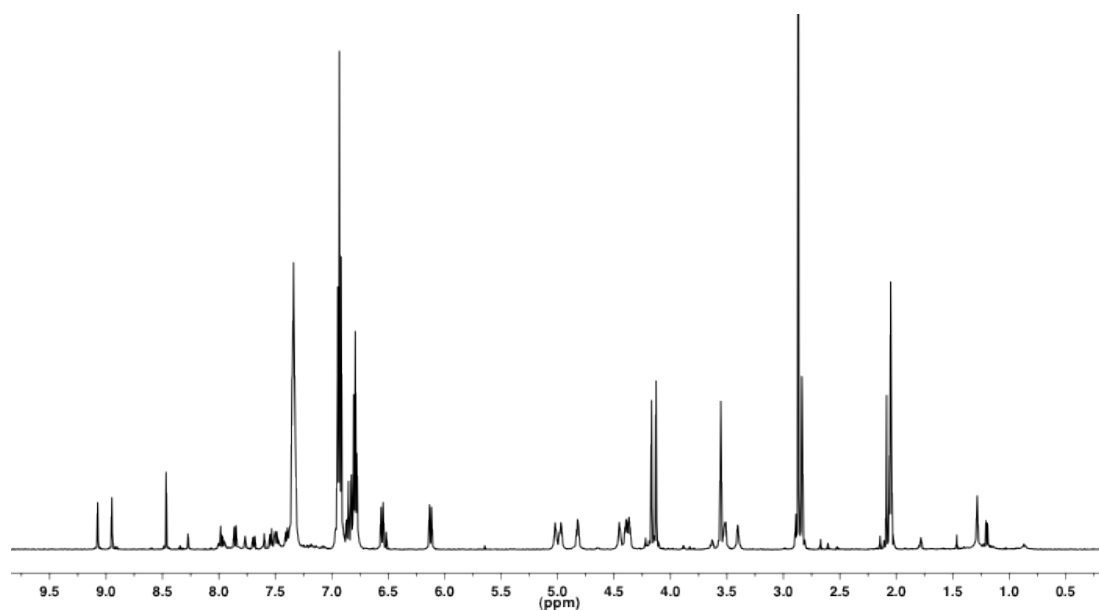


Figure S35. ¹H NMR spectrum of **26**·(BPh₄)₄ (d₆-acetone, 293 K, 500 MHz).

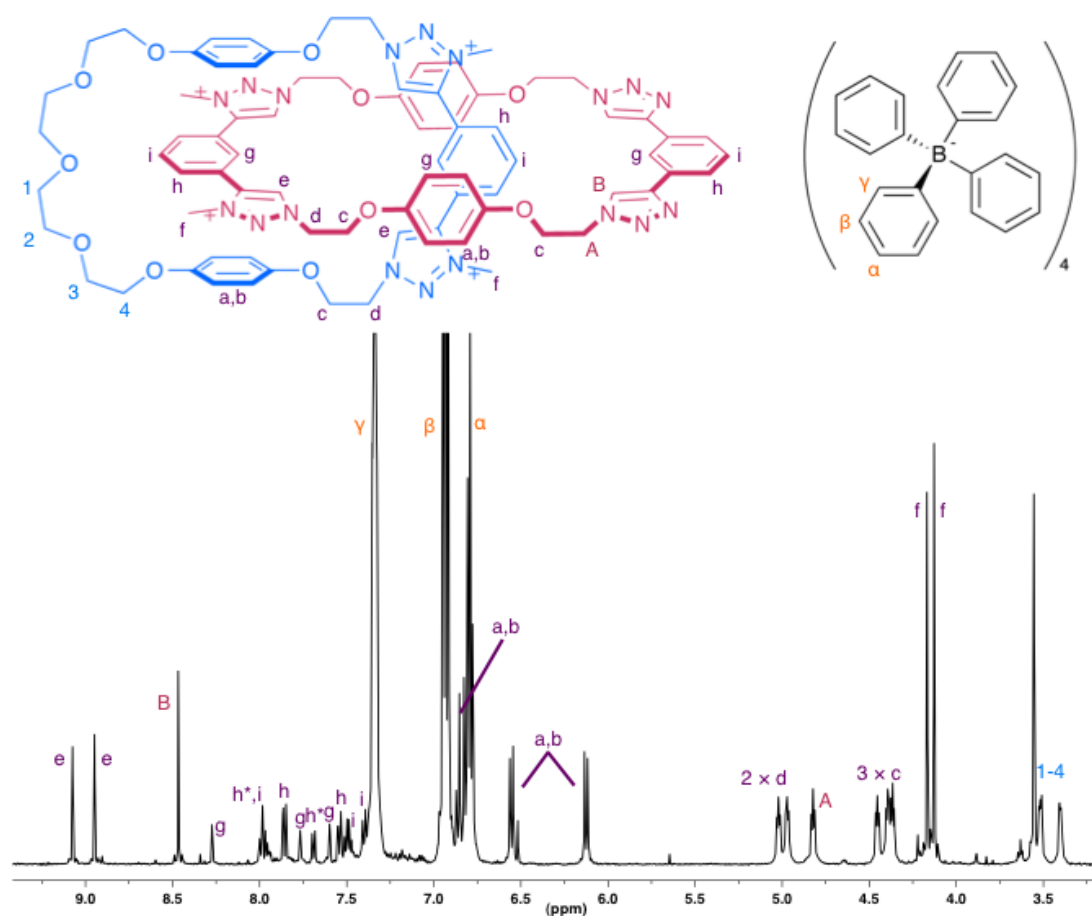
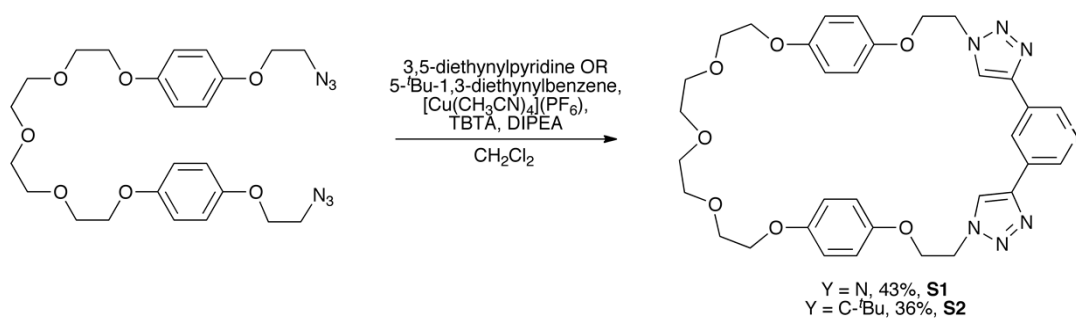


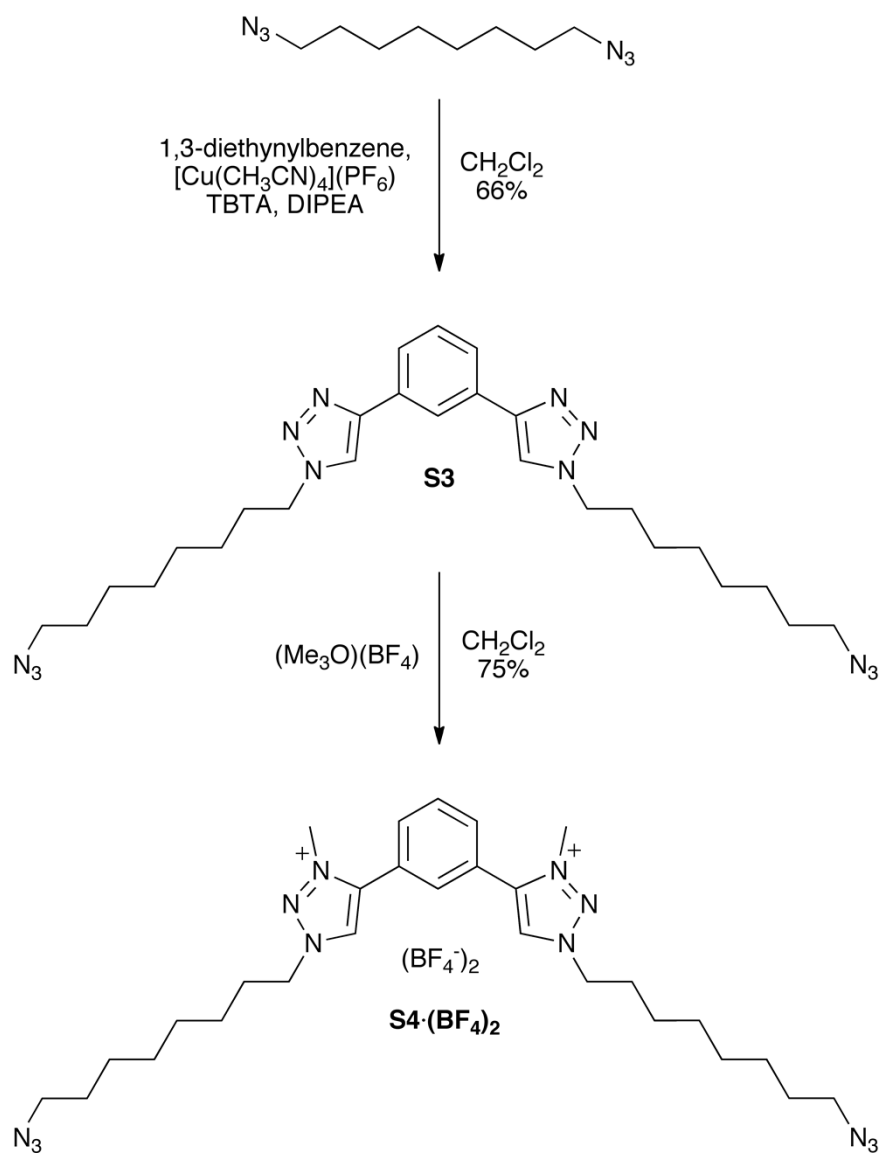
Figure S36. Truncated and labelled ¹H NMR spectrum of **26**·(BPh₄)₄ (d₆-acetone, 293 K, 500 MHz). Peaks that could belong to either macrocyclic component are labelled purple. In one case, the two *h* environments appear to be inequivalent, these have been labelled *h**.

Due to the similar chemical environments of a number of signals, it is not possible to distinguish between them (*e.g.* it is not possible to say which of the two triazolium resonances *e* belongs to which macrocycle). Despite this, and despite the slight impurities present, all proton resonances can be reasonably assigned, which along with the high resolution ESI mass spectrometry data confirm the identity of the tetra-triazolium catenane.

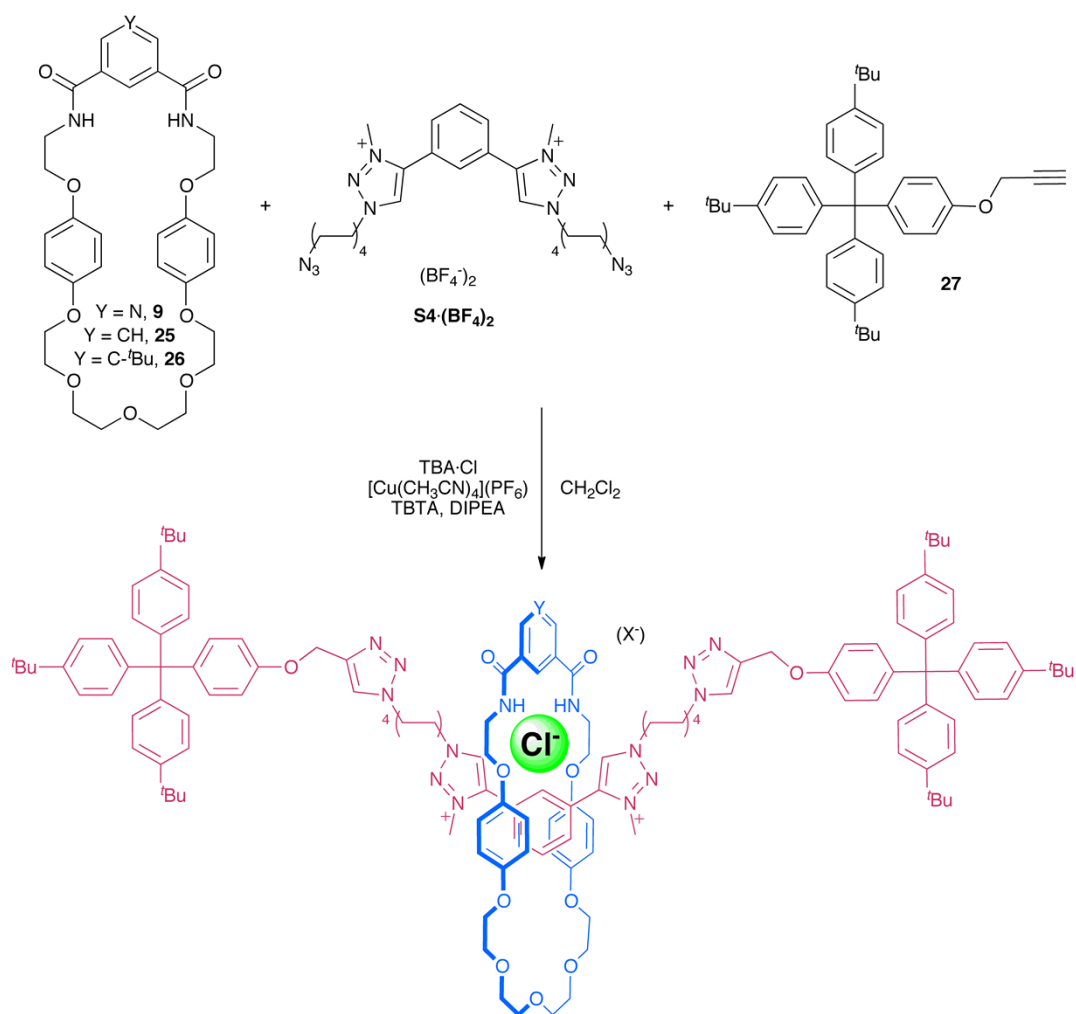
Synthesis and characterisation of additional compounds



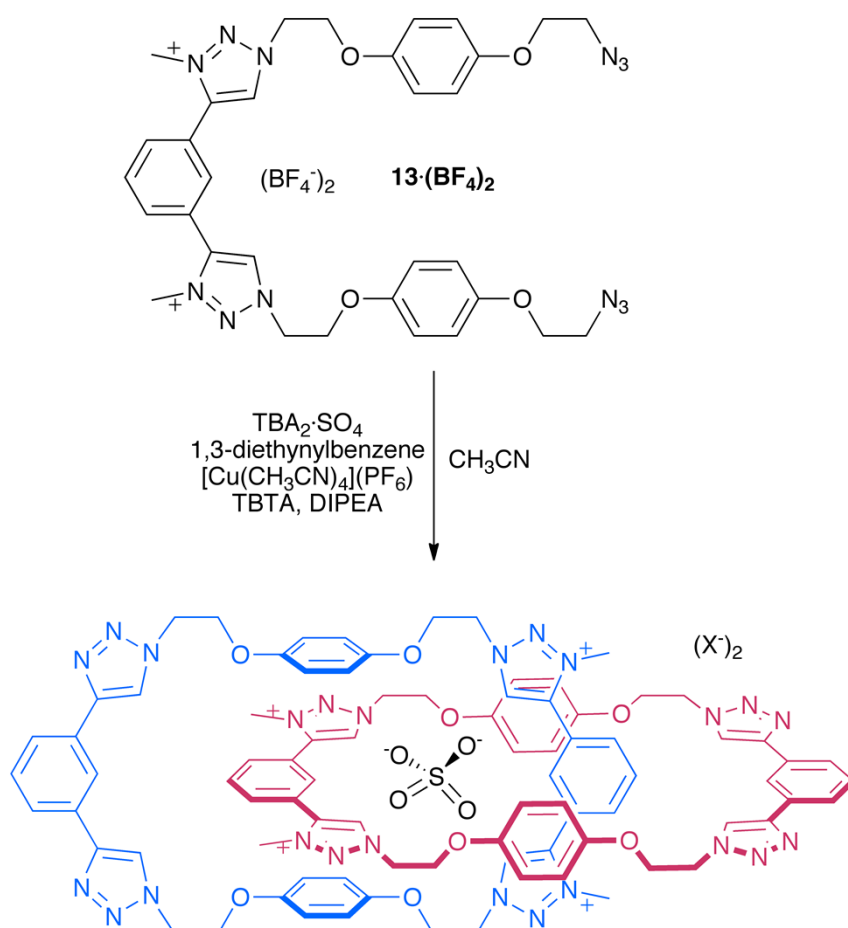
Scheme S1. Synthesis of bis-triazole macrocycles **S1** and **S2**.



Scheme S2. Synthesis of bis(triazolium octyl azide) **S4·(BF₄)₂**.



Scheme S3. Attempted synthesis of octyl-containing bis-triazolium rotaxanes (rotaxanes appeared to be formed in ~ 25% yield, but could not be separated from by-products).



Scheme S4. Attempted synthesis of *homo*-catenane (catenane appeared to be formed but could not be separated from macrocycle by-products).

General remarks

1,8-Diazidooctane was prepared from 1,8-dibromooctane using NaN_3 in DMSO; 3,5-diethynylpyridine was prepared by deprotecting 3,5-bis(trimethylsilyl)ethynylpyridine^{S1} using KOH in methanol; 5-*n*-butyl-1,3-diethynyl benzene was prepared as previously described.^{S2,S3}

Pyridyl macrocycle S1

The bis-azide **1** (0.155 g, 0.300 mmol) and 3,5-diethynyl pyridine (0.038 g, 0.30 mmol) were dissolved in CH_2Cl_2 (300 mL); DIPEA (0.17 mL, 0.13 g, 1.0 mmol), TBTA (0.032 g, 0.060 mmol) and $[\text{Cu}(\text{CH}_3\text{CN})_4](\text{PF}_6)$ (0.022 g, 0.060 mmol) were added and the reaction stirred at room temperature under a nitrogen atmosphere for 3 days. It was taken to dryness under reduced pressure and purified by preparative TLC (4% CH_3OH in CHCl_3) to give **S1** as a white powder. Yield: 0.082 g (43%).

^1H NMR (CDCl_3): 9.12 (d, $^4J = 2.0$ Hz, 2H, py-*H*), 8.32 (t, $^4J = 2.0$ Hz, 1H, py-*H*), 8.10 (s, 2H, trz-*H*), 6.72–6.81 (m, 8H, hydroquinone-*H*), 4.83 (t, $^3J = 4.7$ Hz, 4H, CH_2 -trz), 4.33 (t, $^3J = 4.7$ Hz, 4H, hydroquinone- CH_2), 4.02 (t, $^3J = 4.8$ Hz, 4H, hydroquinone- CH_2), 3.78 (t, $^3J = 4.8$ Hz, 4H, CH_2), 3.63–3.69 (m, 8H, CH_2). ^{13}C NMR (d_6 -DMSO): 152.9, 152.0, 145.2, 143.5, 129.4, 128.8, 123.3, 115.8, 115.2, 70.0, 69.9, 68.9, 67.5, 67.0, 49.8. HRESI-MS (pos.): 666.2647, calc. for $[\text{C}_{33}\text{H}_{37}\text{N}_7\text{O}_7\cdot\text{Na}]^+ = 666.2647$.

5-*n*-Butylphenyl macrocycle S2

The bis-azide **1** (0.155 g, 0.300 mmol) and 5-*n*-butyl-1,3-diethynyl benzene (0.055 g, 0.30 mmol) were dissolved in CH_2Cl_2 (300 mL); DIPEA (0.17 mL, 0.13 g, 1.0 mmol), TBTA (0.032 g, 0.060 mmol) and $[\text{Cu}(\text{CH}_3\text{CN})_4](\text{PF}_6)$ (0.022 g, 0.060 mmol) were added and the reaction stirred at room temperature under a nitrogen atmosphere for 3 days. It was taken to dryness under reduced pressure and purified by preparative TLC (3% CH_3OH in CH_2Cl_2) to give **S2** as a white powder. Yield: 0.075 g (36%).

^1H NMR (CDCl_3): 8.04 (s, 2H, trz-*H*), 8.02 (d, $^4J = 1.5$ Hz, 2H, ph-*H*), 7.75 (t, $^4J = 1.5$ Hz, 1H, ph-*H*), 6.74–6.81 (m, 8H, hydroquinone-*H*), 4.79 (t, $J = 4.7$ Hz, 4H, CH_2 -trz), 4.31 (t, $J = 4.7$ Hz, 4H, hydroquinone- CH_2), 4.02 (t, $J = 4.8$ Hz, 4H, hydroquinone- CH_2), 3.80 (t, $J = 4.8$ Hz, 4H, CH_2), 3.64–3.73 (m, 8H, CH_2), 1.42 (s, 9H, CH_3). ^{13}C NMR (CDCl_3): 153.8, 152.9, 152.2, 148.1, 130.9, 122.9, 121.3, 120.7,

115.8, 110.1, 70.9, 70.9, 69.8, 68.2, 67.6, 50.3, 35.2, 31.5. HRESI-MS (pos.): 721.3314, calc. for $[C_{38}H_{46}N_6O_7 \cdot Na]^+ = 721.3320$.

Bis(triazole octyl azide) S3

1,8-Diazidooctane (1.37 g, 7.00 mmol) and 1,3-diethynylbenzene (0.093 mL, 0.088 g, 0.70 mmol) were dissolved in CH_2Cl_2 (50 mL). DIPEA (0.25 mL, 0.18 g, 1.4 mmol), TBTA (0.074 g, 0.14 mmol) and $[Cu(CH_3CN)_4](PF_6)$ (0.052 g, 0.14 mmol) were added and the resulting yellow solution stirred at room temperature under a nitrogen atmosphere for 16 hours. It was carefully concentrated under reduced pressure and then purified by column chromatography (2% CH_3OH in $CHCl_3$) to give **S3** (0.24 g, 66%) as a slightly off-white waxy solid.

1H NMR ($CDCl_3$): 8.30 (t, $^4J = 1.6$ Hz, 1H, ph-*H*), 7.85 (s, 2H, trz-*H*), 7.83 (dd, $^3J = 7.7$ Hz, $^4J_{j,k} = 1.6$ Hz, 2H, ph-*H*), 7.49 (t, $^3J = 7.7$ Hz, 1H, ph-*H*), 4.42 (t, $^3J = 7.1$ Hz, 4H, trz- CH_2), 3.25 (t, $^3J = 6.9$ Hz, 4H, CH_2-N_3), 1.92–2.01 (m, 4H, trz- CH_2-CH_2), 1.54–1.63 (m, 4H, $CH_2-CH_2-N_3$), 1.30–1.41 (m, 16H, CH_2). ^{13}C NMR ($CDCl_3$): 147.4, 131.3, 129.5, 125.3, 122.8, 119.9, 51.4, 50.5, 30.3, 28.9, 28.9, 28.8, 26.6, 26.4. HRESI-MS (pos.): 541.3235, calc. for $[C_{26}H_{38}N_{12} \cdot Na]^+ = 541.3235$.

Bis(triazolium octyl azide) S4·(BF₄)₂

The bis(triazole) thread **S3** (0.156 g, 0.300 mmol) was dissolved in dry CH_2Cl_2 (25 mL). $(Me_3O)(BF_4)$ (0.097 g, 0.66 mmol) was added and the mixture stirred at room temperature under a nitrogen atmosphere over the weekend. The reaction was quenched by the addition of CH_3OH (1 mL), and then taken to dryness under reduced pressure. Purification by preparative TLC (10% CH_3OH in CH_2Cl_2) gave **S4·(BF₄)₂** as a very pale yellow oil. Yield: 0.163 g (75%).

1H NMR (d_6 -acetone): 9.11 (s, 2H, trz⁺-*H*), 8.30 (s, 1H, ph-*H*), 8.13 (d, $^3J = 8.3$ Hz, 2H, ph-*H*), 7.98 (t, $^3J = 8.3$ Hz, 1H, ph-*H*), 4.83 (t, $^3J = 7.3$ Hz, 4H, trz⁺-*H*), 4.50 (s, 6H, trz⁺- CH_3), 3.32 (t, $^3J = 6.9$ Hz, 4H, CH_2-N_3), 2.10–2.19 (m, 4H, trz⁺- CH_2-CH_2), 1.55–1.63 (m, 4H, $CH_2-CH_2-N_3$), 1.34–1.51 (m, 16H, CH_2). ^{13}C NMR ($CDCl_3$): 141.8, 132.3, 130.8, 130.5, 129.0, 123.7, 54.2, 51.3, 38.7, 28.9, 28.7, 28.6, 26.5, 25.9 (one resonance not observed). ^{19}F NMR (d_6 -acetone): –151.4 (m). HRESI-MS (pos.): 274.1903, calc. for $[C_{28}H_{44}N_{12}]^{2+} = 274.1900$.

NMR Spectra of S1

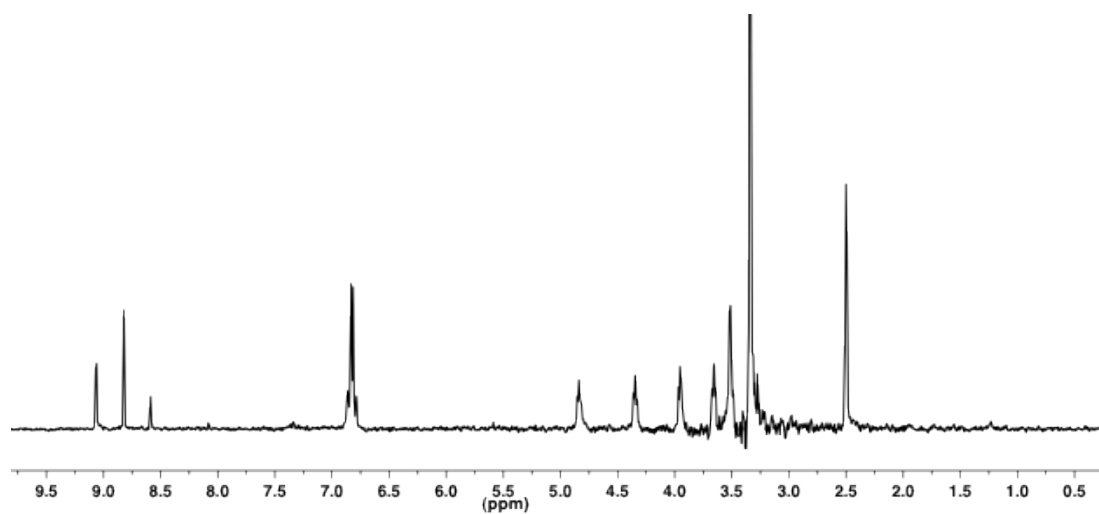


Figure S37. ^1H NMR spectrum of **S1** (d_6 -DMSO, 293 K, 300 MHz).

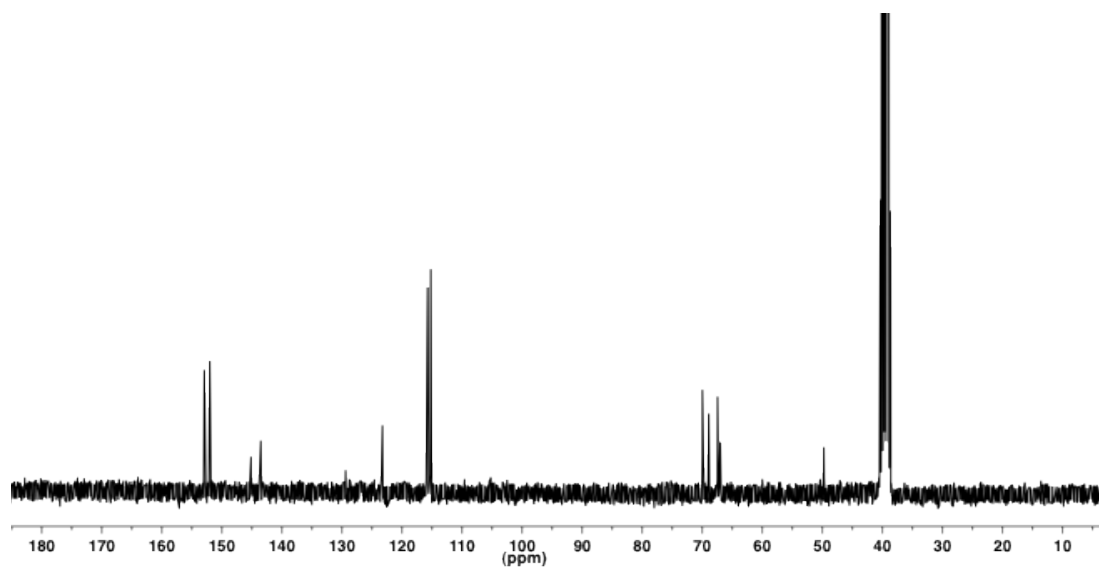


Figure S38. ^{13}C NMR spectrum of **S1** (d_6 -DMSO, 293 K, 76 MHz).

NMR Spectra of S2

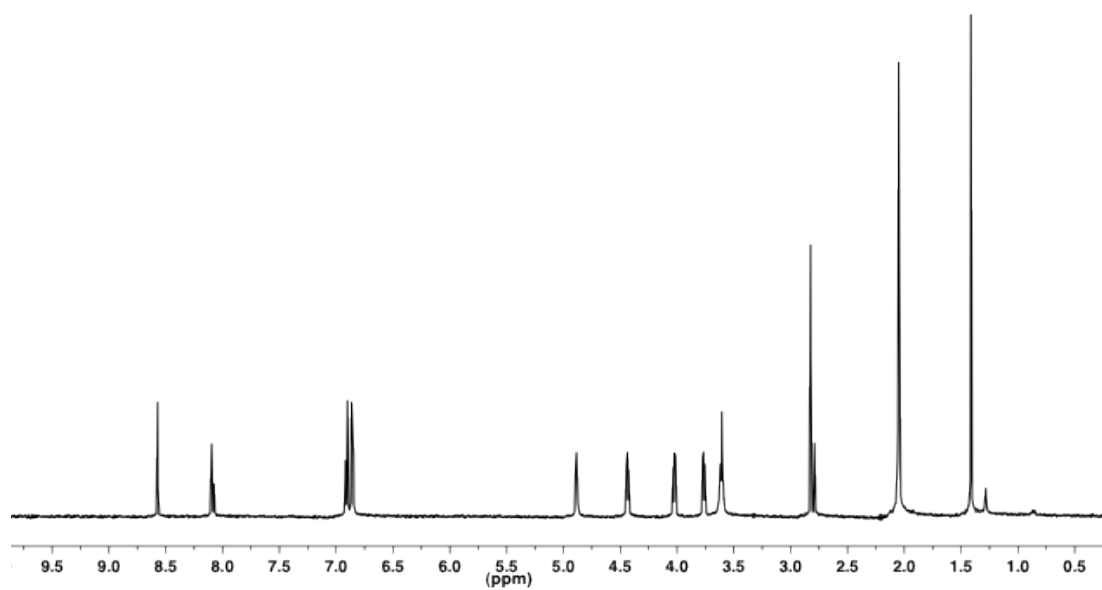


Figure S39. ^1H NMR spectrum of **S2** (d_6 -acetone, 293 K, 500 MHz).

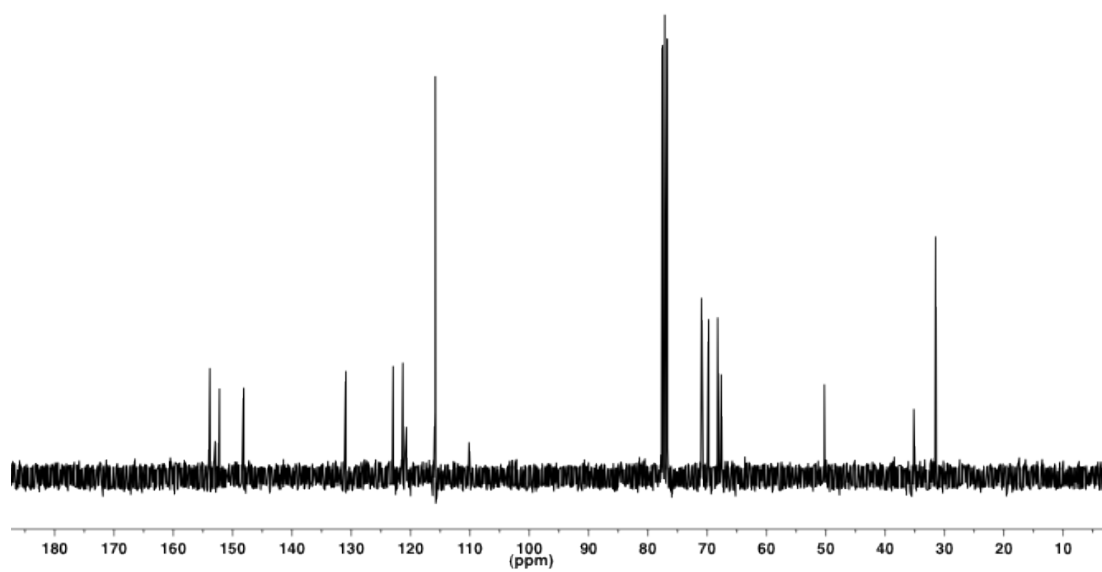


Figure S40. ^{13}C NMR spectrum of **S2** (CDCl_3 , 293 K, 76 MHz).

NMR Spectra of bis(triazole octyl azide) S3

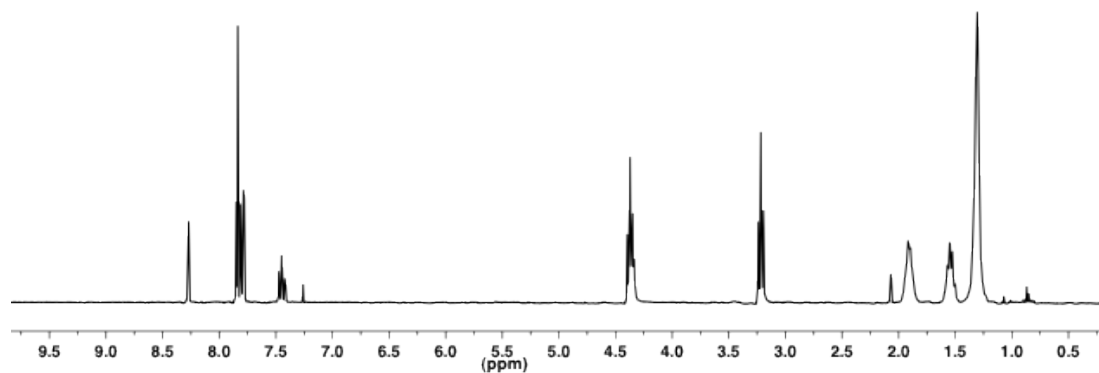


Figure S41. ^1H NMR spectrum of S3 (CDCl_3 , 293 K, 300 MHz).

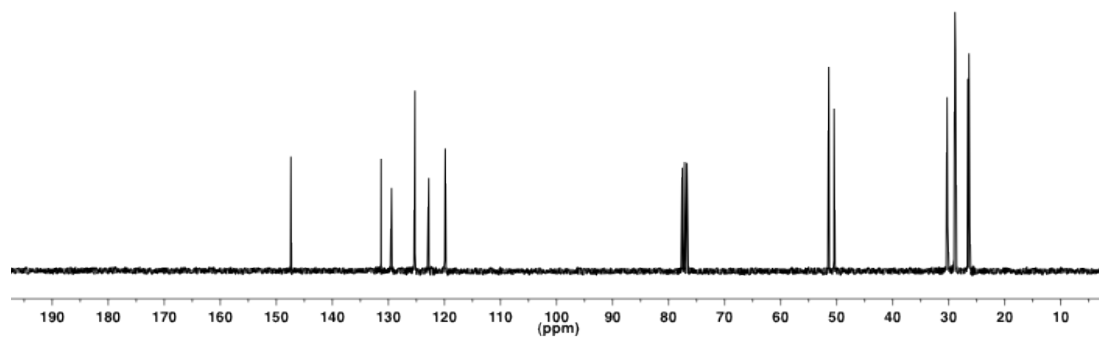


Figure S42. ^{13}C NMR spectrum of S3 (CDCl_3 , 293 K, 76 MHz).

NMR Spectra of bis(triazolium octyl azide) $S4 \cdot (BF_4)_2$

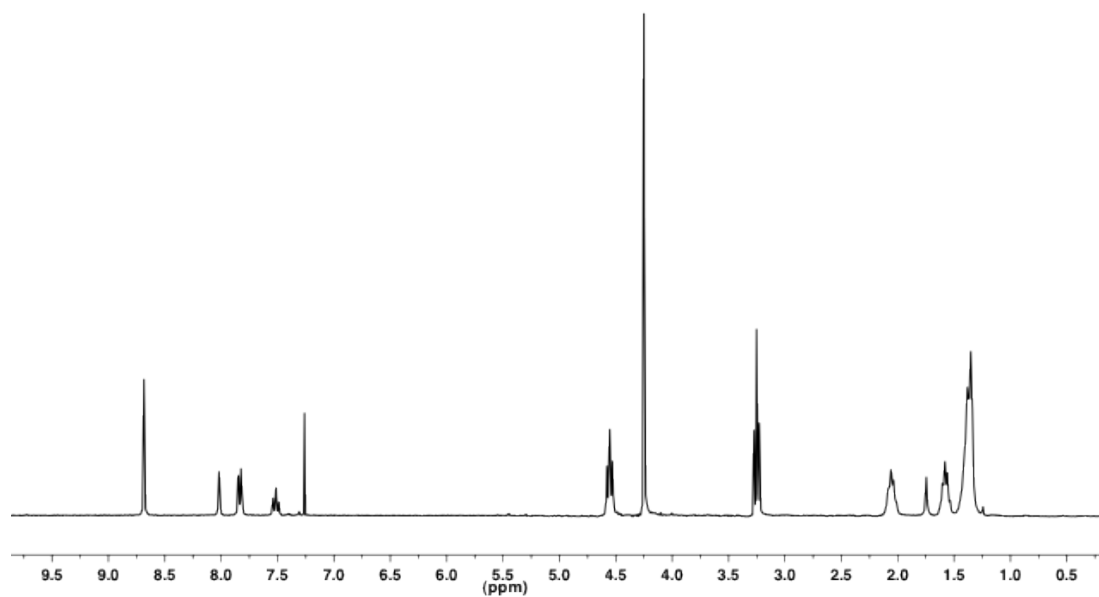


Figure S43. 1H NMR spectrum of $S4 \cdot (BF_4)_2$ ($CDCl_3$, 293 K, 300 MHz).

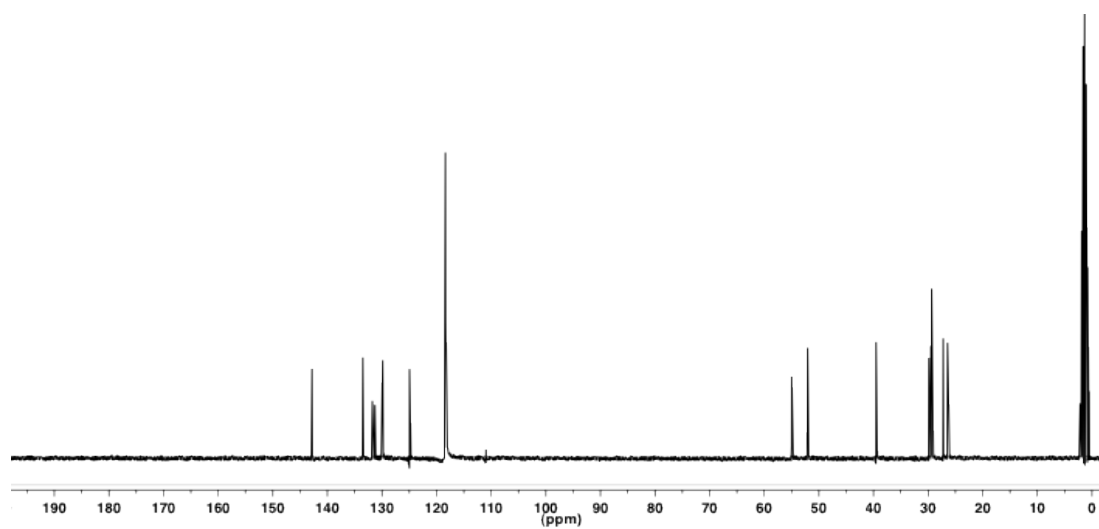


Figure S44. ^{13}C NMR spectrum of $S4 \cdot (BF_4)_2$ (CD_3CN , 293 K, 76 MHz).

Solid state structure of S1

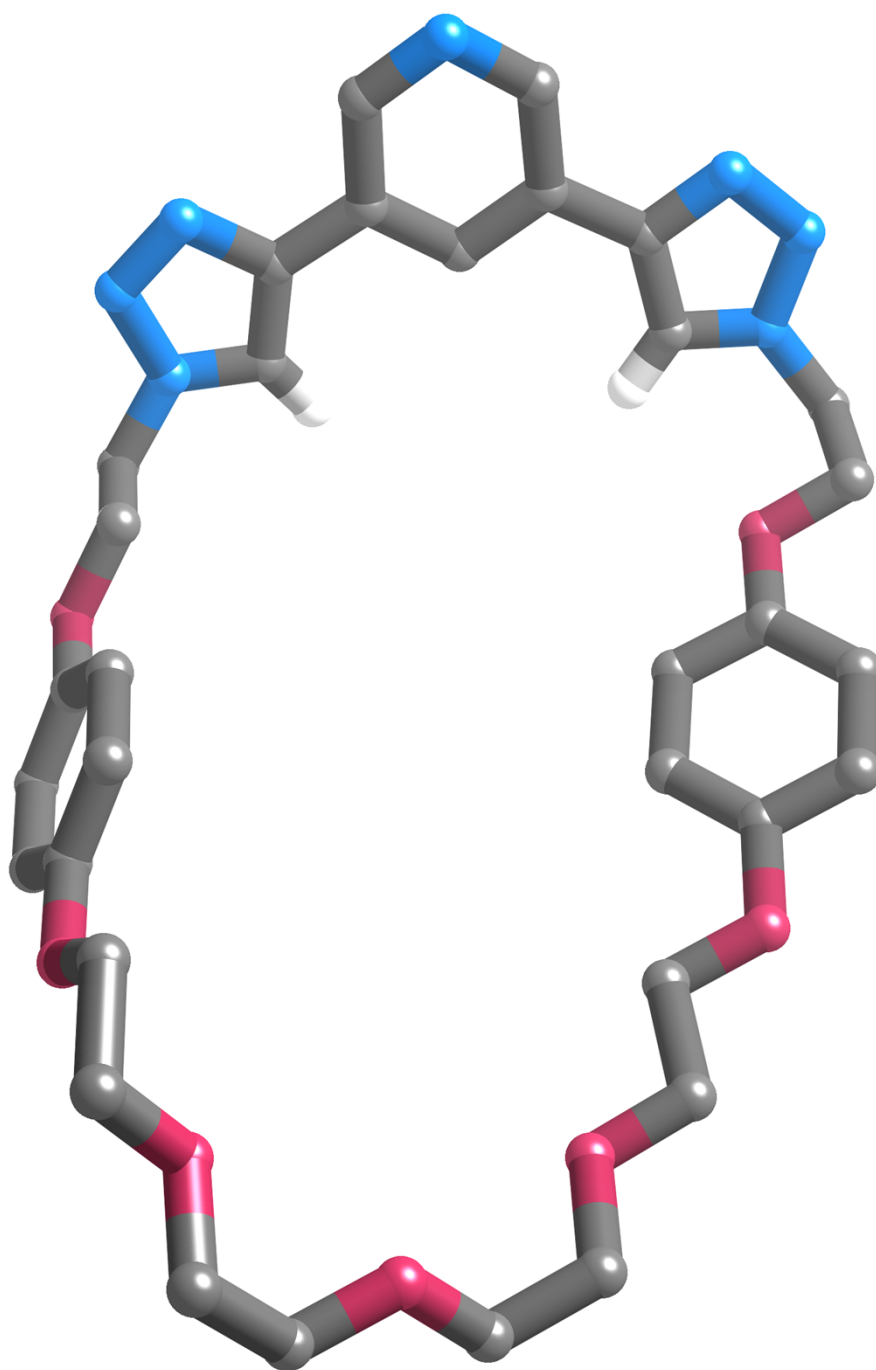


Figure S45. Solid state structure of **S1** (hydrogen atoms and solvent molecules omitted for clarity).

ROESY NMR Spectra of $8 \cdot \text{Cl} \cdot 10$, $5 \cdot \text{SO}_4 \cdot 8$ and $22 \cdot (\text{PF}_6)_2$

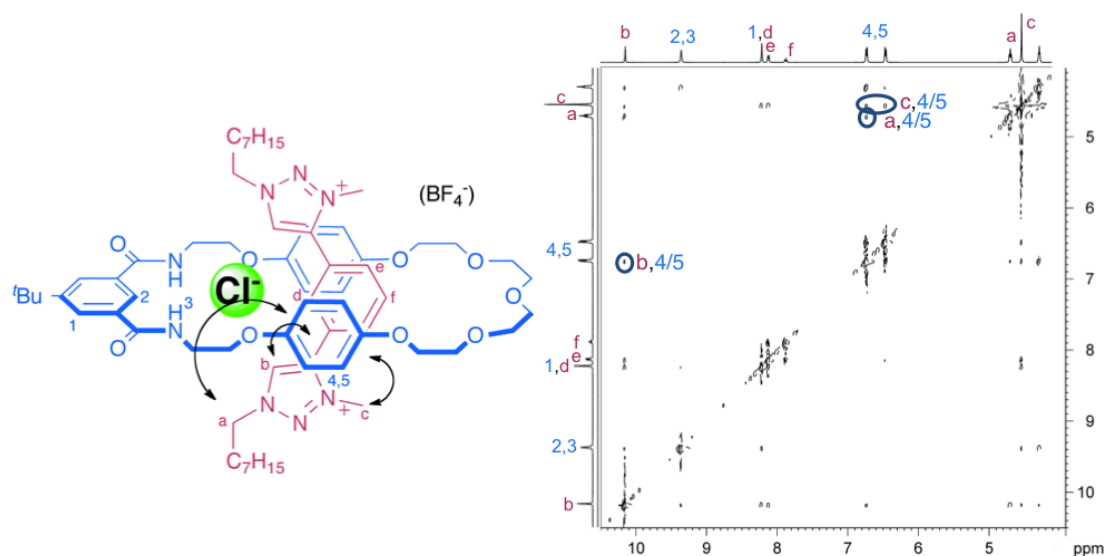


Figure S46. Truncated ROESY NMR spectrum of a 1:1:1 mixture of $8 \cdot (\text{BF}_4)_2$, **10** and TBA·Cl showing selected inter-component couplings (d_6 -acetone, 293 K, 500 MHz).

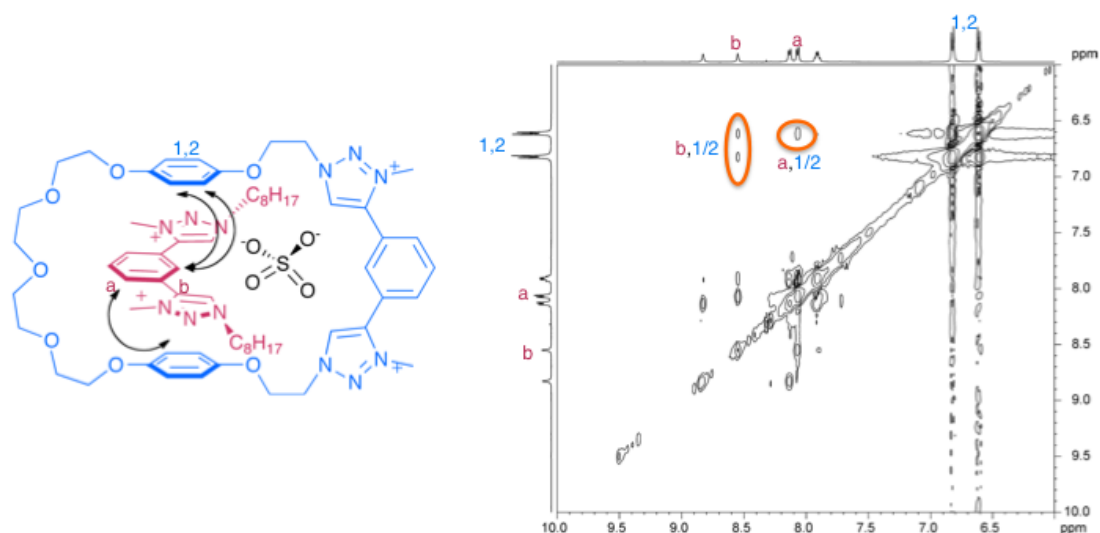


Figure S47. Truncated ROESY NMR spectrum of a 1:1:1 mixture of $5 \cdot (\text{BF}_4)_2$, $8 \cdot (\text{BF}_4)$ and TBA· SO_4 showing selected inter-component couplings (d_6 -DMSO, 293 K, 500 MHz).

Titration protocols and additional binding isotherms

Spectra for ^1H NMR titrations were recorded at 293 K on a Varian Unity Plus 500 spectrometer with ^1H operating at 500 MHz. Initial sample volumes were 0.50 mL and concentrations were 2.0 mM of host. Solutions (100 mM) of anions as their tetrabutylammonium salts were added in aliquots, the samples thoroughly shaken and spectra recorded. Spectra were recorded at 0, 0.2, 0.4, 0.6, 0.8, 1.0, 1.2, 1.4, 1.6, 1.8, 2.0, 2.5, 3.0, 4.0, 5.0, 7.0 and 10 equivalents. Stability constants were obtained by analysis of the resulting data using the WINEQNMR2^{S4} computer program, monitoring the triazole C–H proton resonance in all cases.

Estimates for the association constant and the limiting chemical shifts were added to the program's input file. The parameters were refined by non-linear least-squares analysis using WINEQNMR2^{S4} to achieve the best fit between observed and calculated chemical shifts. The input parameters for the final chemical shift and association constant were adjusted based on the program output until convergence was reached. Comparison of the calculated and experimental binding isotherms demonstrated that an appropriate model with an appropriate 1:1 binding stoichiometry was being used. The 1:1 stoichiometry was also confirmed using approximations of Job plots. A graph of $\Delta\delta \cdot \chi_{\text{H}}$ against χ_{H} was plotted, with a 1:1 binding stoichiometry corresponding to a maximum $\delta \cdot \chi_{\text{H}}$ of approximately 0.5 (χ_{H} = mole fraction of host, $\Delta\delta$ = change in chemical shift relative to free host).

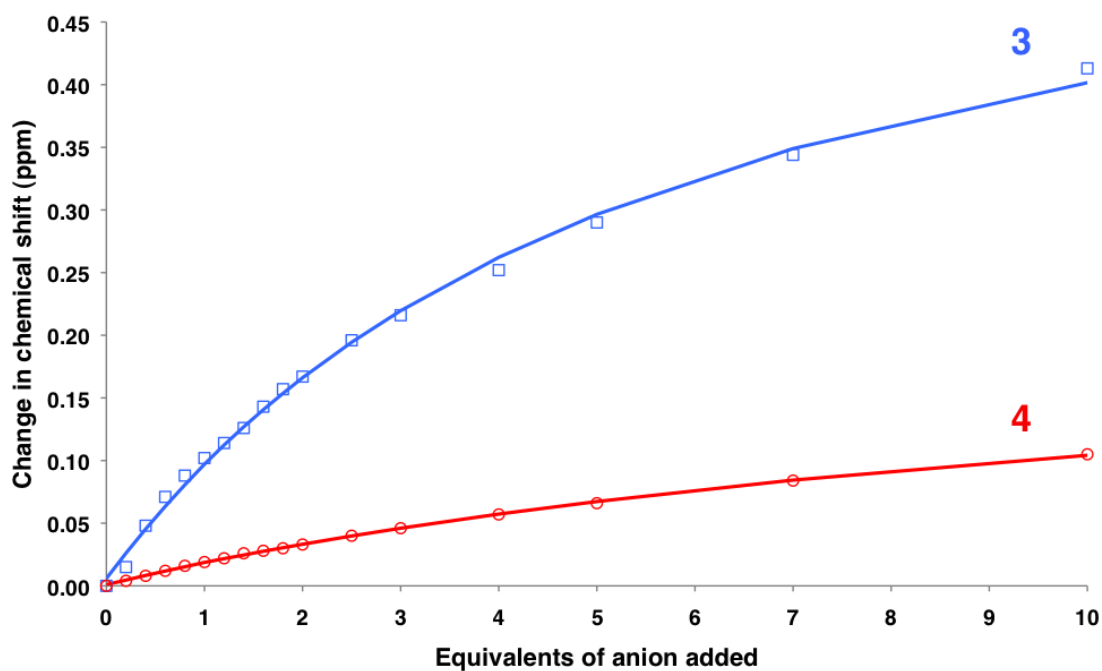


Figure S49. Change in chemical shift of triazole proton of **3** and **4** upon addition of chloride anion. Circles represent data points, lines represent binding isotherms calculated using WINEQNMR2^{S4} (d_6 -acetone, 293 K).

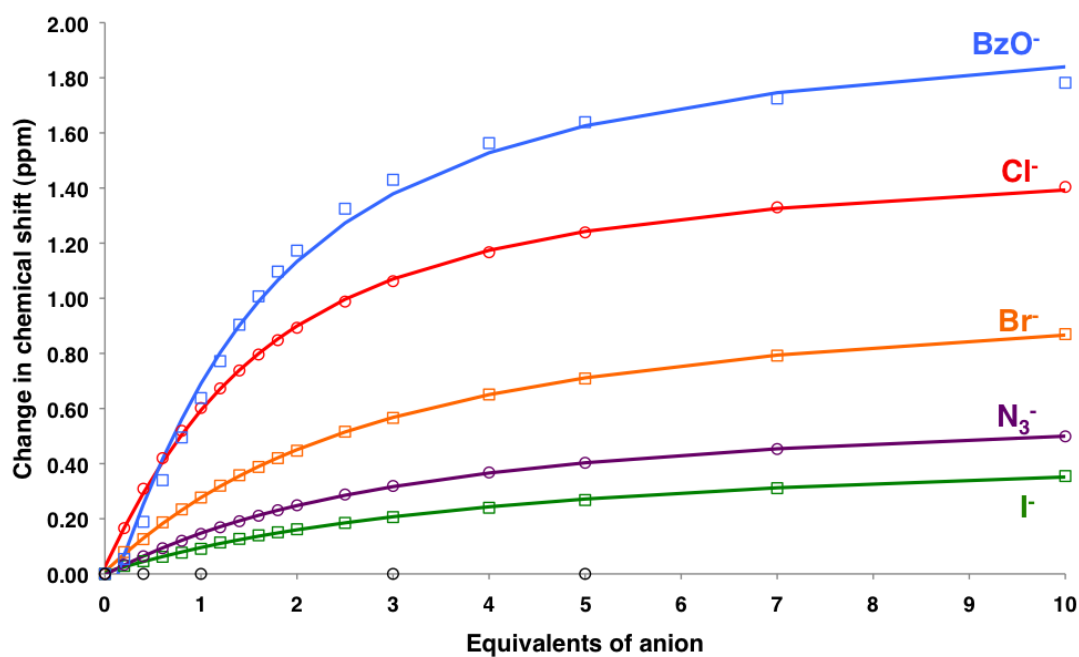


Figure S50. Change in chemical shift of triazolium proton of **5**²⁺ upon addition of anions. Circles represent data points, lines represent binding isotherms calculated using WINEQNMR2^{S4} (CD_3CN , 293 K).

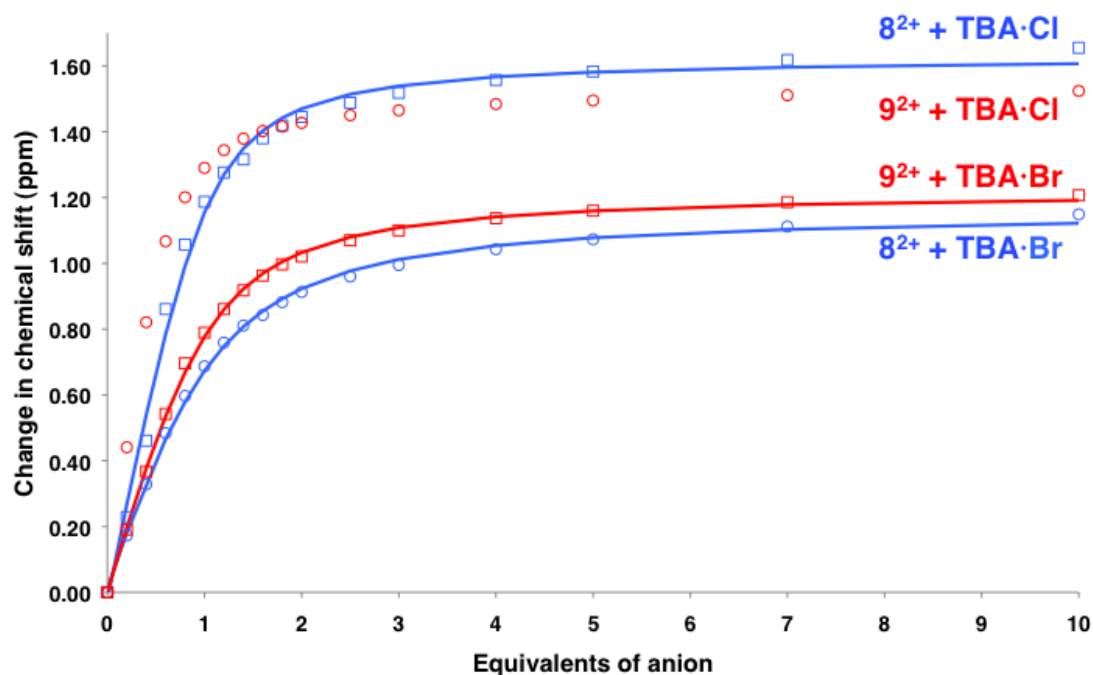


Figure S51. Change in chemical shift of triazolium proton of 8^{2+} and 9^{2+} upon addition of anions. Circles represent data points, lines represent binding isotherms calculated using WINEQNMR2^{S4} (d_6 -acetone, 293 K).

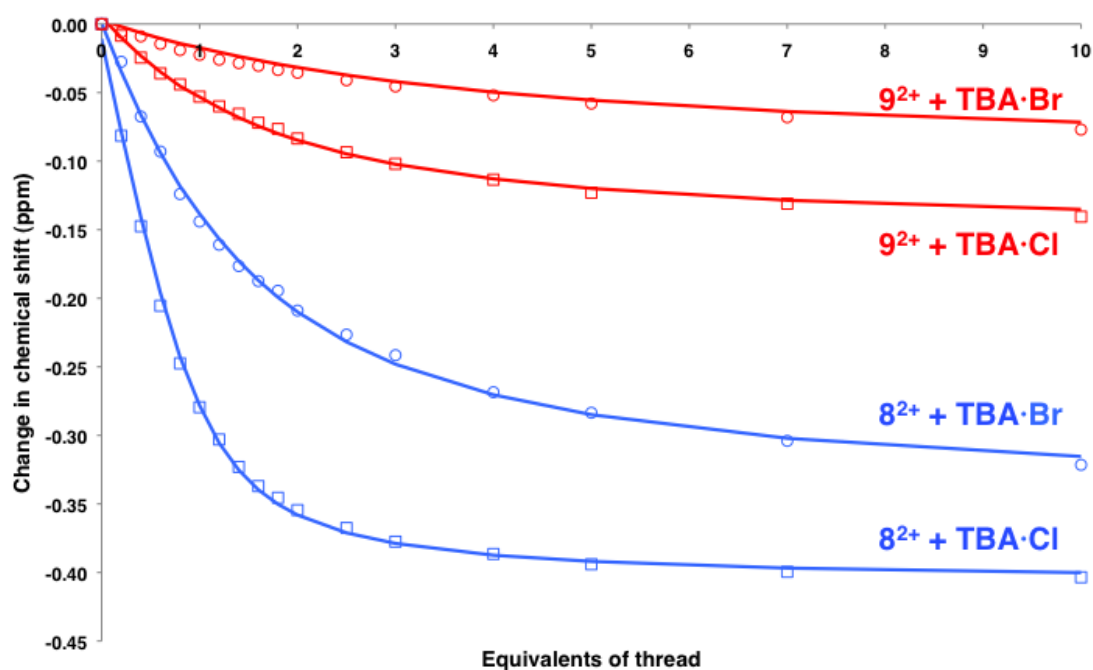


Figure S52. Change in chemical shift of hydroquinone resonance of **10** upon addition of either $8 \cdot (\text{BF}_4)_2$ and one equivalent of TBA·anion or $9 \cdot (\text{BF}_4)_2$ and one equivalent of TBA·anion. Circles represent data points, lines represent binding isotherms calculated using WINEQNMR2^{S4} (anion = Cl⁻ or Br⁻, d_6 -acetone, 293 K).

Comments on X-ray crystallography

For several of the structures presented, it was only possible to grow small and/or thin single crystals of the macrocycles, and these crystals often diffracted weakly. In these cases, synchrotron radiation or Cu radiation and long exposure times were used, but data were often weak. Nevertheless, the overall structure of the macrocycles and macrocycle–anion complexes is clear.

In some cases poorly-resolved areas of electron density, presumably arising from ill-defined solvent molecules, was present. Where this could not be modelled satisfactorily, PLATON-SQUEEZE^{S5,S6} was used to include the electron density in the refinement.

Specific details for each structure are given in the CIF file.

References

- ^{S1} H. Goto, J. Heemstra, D. Hill and J. Moore, *Org. Lett.*, 2004, **6**, 889.
- ^{S2} Y. Tobe, J. Kishi, I. Ohki and M. Sonoda, *J. Org. Chem.*, 2003, **68**, 3330.
- ^{S3} D.A. Shultz, H. Lee, R. Kumar and K.P. Gwaltney, *J. Org. Chem.*, 1999, **64**, 9124.
- ^{S4} M.J. Hynes, *J. Chem. Soc., Dalton Trans.*, 1993, 311.
- ^{S5} P. van der Sluis and A. L. Spek, *Acta Crystallogr.* 1990, **A46**, 194.
- ^{S6} A. Spek, *J. Appl. Crystallogr.*, 2003, **36**, 7.